UNIVERSIDADE FEDERAL DE MINAS GERAIS

Programa de Pós-Graduação em Engenharia Metalúrgica, Materiais e de Minas

Dissertação de Mestrado/Master of Science Research Report

Autor/Author: Dalila Chaves Sicupira

Orientador/Supervisor: Prof. Marcelo Borges Mansur

"Remoção de manganês de drenagem ácida de mina utilizando carvão de osso."

"Removal of manganese from acid mine drainage using bone char."

February/2012.

UNIVERSIDADE FEDERAL DE MINAS GERAIS
Programa de Pós-Graduação em Engenharia Metalúrgica, Materiais e de Minas

Dalila Chaves Sicupira

"Remoção de manganês de drenagem ácida de mina utilizando carvão de osso."

"Removal of manganese from acid mine drainage using bone char."

Dissertação de Mestrado apresentada ao Programa de Pós-Graduação em Engenharia Metalúrgica, Materiais e de Minas da Universidade Federal de Minas Gerais

Área de concentração: Tecnologia Mineral
Orientador: Prof. Marcelo Borges Mansur

Belo Horizonte
Escola de Engenharia da UFMG
February, 2012.

ACKNOWLEDGEMENTS

Initially I would like to thank God for the grace to get here.

My mother, for love, force and unconditional support. To my brother, my boyfriend and all my family, those have always believed in me.

Prof. Marcelo Borges Mansur the opportunity, friendship and learning.

My colleagues Ana Cláudia, Ana Paula, Carolina, Douglas, Eduardo, Emily, José Alberto, Joyce, Leandro, Marcela, Marcos, Michele, Ronie, Sara and Thiago, for companionship and friendship.

People from Laboratory of corrosion, chemical analysis and Metallography.

Financial support from FAPEMIG, CNPq, CAPES and INCT-Acqua: National Institute of Science and Technology of Mineral Resources, Water and Biodiversity.

Bone Char do Brasil Ltda as well as Prof. Sônia Denise Ferreira Rocha (DEMIN/UFMG) and Prof. Ana Cláudia Ladeira (CDTN) for the fruitful discussion and contribution.

Techs. Ilda, Isabel, Andréia, Cláudia and Patrícia.

Profs. Dagoberto Brandão, Vicente Buono, Edwin Auza, Virgínia Ciminelli, Wander Luiz Vasconcelos, Paulo Roberto Brandão, Adriana França, Leandro Oliveira and Maria Silvia for the analysis.

PPGEM: Cida and Nelson.

Ultimately, I thank all those who directly or indirectly contributed to the realization of this work.

SUMMARY

LIST OF FIGURES

LIST OF TABLES

RESUMO

Um estudo em batelada e em leito fixo foi realizado com o objetivo de avaliar a viabilidade do uso de carvão de osso na remoção de manganês presente em efluentes de drenagem ácida de mina (DAM). Ensaios com solução sintética contendo apenas manganês também foram realizados para fins de comparação. Testes de equilíbrio revelaram que a capacidade máxima de adsorção de manganês baseada na equação de Langmuir foi de 22 mg g^{-1} para o efluente e 20 mg g^{-1} para a solução sintética. A cinética de adsorção de manganês em carvão de osso foi descrita pelo modelo de pseudo-segunda ordem. A remoção de manganês foi influenciada pelas variáveis operacionais razão sólido/líquido e pH da fase aquosa, sendo favorecida em valores de pH próximos da neutralidade. O efeito do tamanho das partículas e da temperatura foi não significativo para a faixa investigada. A difusão intrapartícula revelou-se a principal etapa limitante para a adsorção de manganês, mas a difusão da camada limite também pode afetar sua remoção em partículas menores. As seguintes variáveis operacionais foram avaliadas nos testes contínuos em leito fixo: massa de carvão de osso, vazão e pH inicial. Variações significativas na resistência à transferência de massa de manganês no carvão de osso foram identificadas utilizando o modelo de Thomas. Efeito significativo da massa de adsorvente foi observado apenas em testes com a solução sintética. Nenhuma mudança significativa no volume de ruptura foi observada para diferentes vazões. Aumentando-se o pH inicial de 2,96 para 5,50, o volume de trespasse foi aumentado. A capacidade máxima de adsorção de manganês calculado em testes contínuos foi 6,03 mg g^{-1} para o efluente e 26,74 mg g^{-1} para solução sintética. O estudo incluiu também testes de dessorção utilizando soluções de HCl, H_2SO_4 e água, mas resultados não promissores foram obtidos devido aos baixos níveis de dessorção associados a elevada perda de massa. Apesar disso, a remoção de manganês de efluentes de DAM usando carvão de osso como adsorvente é tecnicamente viável, atendendo a legislação ambiental. É interessante notar que utilizando carvão de osso para remover o manganês pode-se evitar a necessidade de correção do pH do efluente pós-tratamento com cal. Além disso, ele pode remover íons flúor e outros metais, sendo um material alternativo bastante interessante para tal aplicação.

Palavras-chave: manganês; carvão de osso; drenagem ácida de mina; coluna de leito fixo; adsorção/dessorção.

ABSTRACT

Batch and continuous fixed bed tests were carried out aiming to evaluate the feasibility of using bone char for the removal of manganese from acid mine drainage (AMD). Tests with laboratory solution containing solely manganese at typical concentration levels were also carried out for comparison purposes. Equilibrium tests revealed that Langmuir based maximum manganese uptake capacity was 22 mg g^{-1} for AMD effluent and 20 mg g^{-1} for laboratory solution. Manganese kinetics onto bone char was best described by the pseudo-second order model. Manganese removal was influenced by operating variables solid/liquid ratio and pH of the aqueous phase, and it was favored at nearly neutral pH values. The effect of particle size and temperature was not significant for the operating range investigated. It has been found that intraparticle diffusion is the main rate-limiting step for manganese sorption systems but additional contribution from boundary layer diffusion might also affect removal when bone char particles of smaller sizes are used. The following operating variables were evaluated for continuous fixed bed tests: mass of bone char, flow rate and initial pH. Significant variations in resistance to the mass transfer of manganese into the bone char were identified using the Thomas model. A significant effect of bed height was observed only in tests with laboratory solution. No significant change on the breakthrough volume was observed with different flow rate. Increasing the initial pH from 2.96 to 5.50, the breakthrough volume was increased. The maximum manganese loading capacity calculated in continuous tests using bone char for AMD effluent was 6.03 mg g^{-1} and for laboratory solution was 26.74 mg g^{-1}. The study included also desorption tests using solutions of HCl, H_2SO_4 and water but no promising results were obtained due to low desorption levels along with relatively high mass loss. Despite of this, the removal of manganese from AMD effluents using bone char as adsorbent is technically feasible thus attending environmental legislation. It is interesting to note that the use of bone char for manganese removal may avoid the need for pH correction of the effluent after treatment with lime. Also, it can remove fluoride ions and other metals, so bone char is a quite interesting alternative material for the treatment of AMD effluents**.**

Key-words: manganese; bone char; acid mine drainage; continuous fixed bed column; adsorption/desorption.

1. INTRODUCTION

Given its dynamics and persistence, acid mine drainage (AMD) is one of the most serious environmental problems of mining industry. Such phenomenon occurs when pyrite and other sulfide minerals are oxidized due to its exposure to oxygen and water, producing sulfuric acid and dissolved metals (Nascimento, 1998). The main sources of AMD are open pit or underground mines, waste rock piles, tailings storage and ore stockpiles. The raise in the concentration of metal ions in the water due to AMD is an important source of contamination of watercourses, especially when ions can be spread to the food chain. Aiming to minimize the severity of such impacts, environmental protection laws require appropriate plans for mine closure as an attempt to increase the cycle life of closed mines including steps of decommissioning and recovery of degraded areas (Gonçalves, 2006).

A significant increase in the concentration of metal ions in water due to AMD represents an important source of contamination of watercourses, especially when ions can be spread to the food chain. In addition, many wastes containing heavy metals have high contamination power, which can easily reach reservoirs and rivers that are sources of water supply for the cities (Gonçalves, 2006).

In Brazil, the problem of acid mine drainage has been highlighted in coalfields in the south of the country and in the Industrial Mining Complex of Poços de Caldas (CIPC), Nuclear Industries of Brazil, INB. In this latter area there are two watersheds, Ribeirão das Antas and Rio Verde. The waters of this region are mainly used for agricultural irrigation and watering cattle, and also the practice of fishing. Within a radius of 20 km, is not observed any domestic use of these waters (Gonçalves, 2006). Currently, the industrial complex remains disabled and in process of decommissioning.

In CIPC, a large quantity of waste consisted mainly of uranium was produced and it was disposed in large areas surrounding the mined area, called “bota-fora”. Until July 1996, CIPC had processed 2.111.920 tons of ore (dry basis) which resulted in the generation of 44.56 million m^3 of wastes from mining (Nascimento, 1998).

These areas becames a source of acid mine drainage containing radionuclides (uranium, thorium and radium) and stable elements (manganese, zinc, fluoride, iron, etc.) at concentration levels above those allowed by Brazilian legislation for direct discharge into the environment (Gonçalves, 2006; CONAMA, 2005). The current treatment of acid waters consists of metals precipitation with lime, but manganese ions are notoriously difficult to remove from AMD due to their complex chemistry (Bamforth *et al*., 2006; Robinson-Lora and Brennan, 2010a). For complete precipitation, pH around 11 is required, which makes the consumption of lime to be around 350 tons per month (Gonçalves, 2006).

Therefore, new technologies to minimize the environmental impacts of mineral processing operation are urged. Among them, metals adsorption process has been investigated (Korn *et al*., 2004; Soto *et al.*, 2005; Bosco *et al*., 2005), however relatively little attention has been directed to manganese removal. The use of adsorption in hydrometallurgical processes has many advantages, since it allows the recovery of metal ions from very dilute solutions and it has also the ability to process large volumes of solutions where others operations would be unfavorable. In this context, the study of manganese removal by adsorption process is justified, because the environmental impact of the CIPC can be reduced with the advantage to drastically reduce the lime consumption as well.

Bone char can be successfully applied for metals removal (Pan *et al.*, 2009; Choy *et al*., 2004). This material has been used as an alternative material to remove several metals, such as copper, zinc, cadmium, arsenic, mercury, etc (Choy *et al*., 2004; Chen *et al*., 2008; Cheung *et al*., 2000; Hassan *et al*., 2008), however the use of bone char in the manganese removal has little information until date.

In the view of the aforementioned, the aim of this work is to evaluate the feasibility of using bone char in the treatment of AMD containing manganese in order to reach the levels required by the Brazilian legislation for direct discharge into the environment (CONAMA, 2005) which limits the total dissolved Mn concentration in the effluent to 1 mg L^{-1}.

1.1. References

ANNADURAI, G., LING, L.Y., LEE, J.F., 2008. Adsorption of reactive dye from solution by chitosan: isotherm, kinetic and thermodynamic analysis. *Journal of Hazardous Materials*, 152, 337-346.

BAMFORTH, S.M., MANNING, D.A.C., SINGLETON, I., YOUNGER, P.L., JOHNSON, K.L., 2006. Manganese removal from mine waters - investigating the occurrence and importance of manganese carbonates. *Applied Geochemistry*, 21, 1274-1287.

BOSCO, S.M.D., JIMENEZ, R.S., CARVALHO, W.A., 2005. Removal of toxic metals from wastewater by Brazilian natural scolecite. *Journal of Colloid and Interface Science*, 281, 424-431.

CHEN, Y.-N., CHAI, L.-Y., SHU, Y.-D., 2008. Study of arsenic(V) adsorption on bone char from aqueous solution. *Journal of Hazardous Materials*, 160, 168-172.

CHEUNG, C.W., PORTER, J.F., MCKAY, G., 2000. Sorption kinetics for the removal of copper and zinc from effluents using bone char. *Separation and Purification Technology*, 19, 55-64.

CHOY, K.K.H., KO, D.C.K., CHEUNG, C.W., PORTER, J.F., MCKAY, G., 2004. Film and intraparticle mass transfer during the adsorption of metal ions onto bone char. *Journal of Colloid and Interface Science*, 271, 284-295.

CONSELHO NACIONAL DO MEIO AMBIENTE. Resolução CONAMA n.º 357/2005: Classificação dos corpos de água e diretrizes ambientais para o seu enquadramento, bem como estabelece as condições e padrões de lançamento de efluentes. Brasília, 2005. Disponível na Web em: http://www.mma.gov.br/port/conama/index.cfm.

GONÇALVES, C.R., 2006. Remoção de manganês e recuperação de urânio presentes em águas ácidas de mina. M.Sci. Thesis, CDTN, Belo Horizonte, Brazil.

KORN, M.G.A., SANTOS JR., A.F., JAEGER, H.V., SILVA, N.M.S., COSTA, A.C.S., 2004. Cooper, zinc and manganese determination in saline samples employing FAAS after separation and preconcentration on Amberlite XAD-7 and Dowex 1X-8 loaded with alizarin Red. *Journal of Brazilian Chemical Society*, 15(2), 212-218.

NASCIMENTO, M.R.L., 1998. Remoção e recuperação de urânio de águas ácidas de mina por resina de troca iônica. M.Sci. Thesis, UFSCar, São Carlos, Brazil.

PAN, X., WANG, J., ZHANG, D., 2009. Sorption of cobalt to bone char: kinetics, competitive sorption and mechanism. *Desalination*, 249, 609-614.

ROBINSON-LORA, M.A., BRENNAN, R.A., 2010a. Biosorption of manganese onto chitin and associated proteins during the treatment of mine impacted water. *Chemical Engineering Journal*, 162, 565-572.

SOTO, O.A.J.; TOREM, M.L.; TRINDADE, R.B.E. Palygorskite as a sorbent in the removal of manganese (II) from water mine effluents. In: XIII INTERNATIONAL CONFERENCE ON HEAVY METALS IN THE ENVIRONMENT, Rio de Janeiro - RJ, 2005.

2. OBJECTIVES

2.1. Main objective

Evaluation of the performance of bone char to treat AMD effluents containing manganese in order to reach the level required by the environmental legislation (i.e., 1 mg L^{-1} according to CONAMA, 2005) for direct discharge into the environment.

2.2. Specific objectives

- Physical and chemical characterizations of the bone char before and after treatment of AMD using analytical techniques such as X-ray diffraction, Fourier transform infrared spectroscopy, Scanning electron microscopy and Braunauer, Emmet e Teller method.
- Study of kinetics of manganese removal and evaluation of the effects of operating parameters solid/liquid ratio and size of particles.
- Evaluation of the isotherms of manganese removal in batch tests and evaluation of the effect of operating parameters pH and temperature.
- Investigation of metal desorption in order to evaluate the ability of sorbent to be recycled and/or the metal to be recovered for reuse.
- Execution of continuous experiments in laboratory columns in order to evaluate the effect of flow rate, mass of bone char and initial pH.

3. BACKGROUND

3.1. Acid mine drainage

Among the main environmental aspects and impacts of mining activities, the one associated with the contamination of surface and ground waters by acid mine drainage (AMD) is probably one of the most significant (Nascimento, 1998). AMD may occur when the metal or mineral of interest is associated with sulfides like pyrite (FeS_2), for example, in the extraction of gold, coal, copper, zinc and uranium. Mining wastes when exposed to oxidizing conditions in the presence of water may result in AMD, therefore the proper disposal of mining wastes from such operations is fundamental to prevent and minimize the generation of AMD (Gonçalves, 2006). Besides waste rock piles, acid mine drainage may also occur in open or underground pit mines, tailings storage and ore stockpiles.

The basic reactions that describe the phenomenon of pyrite oxidation are:

$$2FeS_{2(s)} + 7O_2 + 2H_2O \leftrightarrows 4SO_4^{2-} + 2Fe^{2+} + 4H^+ \quad (3.1)$$

$$4Fe^{2+} + O_2 + 4H^+ \leftrightarrows 4Fe^{3+} + 2H_2O \quad (3.2)$$

$$FeS_{2(s)} + 14Fe^{3+} + 8H_2O \leftrightarrows 2SO_4^{2-} + 15Fe^{2+} + 16H^+ \quad (3.3)$$

$$2Fe^{3+} + 6H_2O \leftrightarrows 2Fe(OH)_{3(s)} + 6H^+ \quad (3.4)$$

According to reaction (3.1), pyrite reacts with oxygen in the presence of water. The ferrous ion then slowly oxidized (reaction 3.2) resulting in ferric iron. The ferric iron formed accelerates the pyrite oxidation according to reaction (3.3), thus increasing the acidity and the concentration of Fe^{2+} that enter in the cycle by reaction (3.2). The precipitated iron hydroxide formed by reaction (3.4) is a reservoir of soluble Fe^{3+} (Nascimento, 1998).

AMD often contains high concentrations of SO_4^{2-} ions and the high acidity may promote the dissolution of metals such as Zn, Cu, Cd, As, Fe, U, Al and Mn from the minerals (Bamforth *et al*., 2006; Robinson-Lora and Brennan, 2009).

Three different processes are required for the treatment of AMD (Robinson-Lora and Brennan, 2009):

- The addition of a neutralizing agent;
- The reduction of sulfate concentrations;
- The removal of dissolved metals.

3.2. Manganese

The industrial applications of manganese included steel alloy, dry cell battery, glass and ceramic, paint, ink, dye and fertilizers (Mohan and Chander, 2006a). Manganese is found in acid mine drainage (AMD) derived from coal and metal mining, and their concentration can vary considerably, from below 1 mg L^{-1} to hundreds of mg L^{-1} in untreated AMD (Robinson-Lora and Brennan, 2010a).

Although it is typically found at lower concentrations in AMD and it has a lower toxicity than most of other metal contaminants, Mn still affects the color, taste, and odor of water (Robinson-Lora and Brennan, 2010a).

Manganese is an important trace element for the functioning and activation of many enzymes (manganese superoxide dismutase, kinases, decarboxylases, among others) in the human body, but at high levels, it causes damage to the brain, liver, kidneys and nervous system (Silva *et al*., 2010). Because of this, discharges from mining activities to surface water in Brazil must comply with the Brazilian environmental legislation (CONAMA, 2005), which limits the total dissolved Mn concentration in the effluent to 1 mg L^{-1}.

In natural systems, manganese can form a number of different solid phases. The main factors that affect the composition of minerals containing Mn are the pH and the Eh of the aqueous system. In an oxidizing environment, Mn oxides are commonly formed,

including Mn oxyhydroxides and phyllomanganates (Lind and Hem, 1993). Mn sulfides such as alabandite are expected to form in reducing environments, at high pH (Bamforth *et al*., 2006). Manganese carbonate minerals such as rhodochrosite ($MnCO_3$) and kutnahorite ($CaMn(CO_3)_2$) have been identified in mine water-impacted environments (Lind and Hem, 1993). Lind and Hem (1993) also suggest that the formation of Mn carbonates in contaminated mine waters may be an essential mechanism for the long-term immobilization of Mn.

The solubility of manganese in water is favored by reducing conditions (Soto *et al*., 2005). In the reduced Mn^{2+} state, Mn is relatively soluble as $MnSO_4^0{}_{(aq)}$ complex at least up to pH 8. At higher pH, it can precipitate as $MnCO_3$ (rhodochrosite) and $Mn(OH)_2$ (at low CO_2 pressure). In contrast, under oxidizing conditions, Mn^{3+} and Mn^{4+} species are relatively insoluble in the form of MnO_2, Mn_2O_3, Mn_3O_4 and related compounds. The removal of Mn from AMD requires either high pH or strong oxidizing conditions (Rose *et al*., 2003a). The neutralized solution, however, requires pH adjustment to the value below 9.0 (CONAMA, 2005) to be discharged.

Rose *et al*. (2003a) showed that if Fe^{2+} is present in solution, Mn cannot precipitate at near-neutral pH. For Mn to precipitate, the water must be well oxygenated to the extent that essentially all Fe is insoluble.

3.3. Technologies for AMD treatment

A number of active and passive treatment technologies (Figure 3.1) have been suggested to remove contaminants from AMD. Although Mn removal is difficult, relatively little attention has been directed to Mn removal systems (Rose *et al*., 2003b).

Active treatment systems are those that use mechanical energy to promote mixing of neutralizing agents with AMD, for example, water treatment stations that use stirred tanks (Johnson and Hallberg, 2005). Typically, active treatment of AMD involves chemical processes by the addition of an alkaline agent and/or sulfide to promote the precipitation of the metals as hydroxides, carbonates, or sulfides (Robinson-Lora and Brennan, 2009). The alkaline reagents, normally used in the conventional neutralization

of pH of AMD (CaO, $CaCO_3$, NaOH, Na_2CO_3) produce a considerable volume of solid waste rich in iron and other metals, whose disposal represents another environmental problem and additional costs. Other limitations of this process can be pointed out, as lack of selectivity of the precipitation process, their constant demand for supplies, energy and maintenance and low efficiency in the remediation of dilute solutions (Laus *et al*., 2005; Robinson-Lora and Brennan, 2010b).

Aziz and Smith (1992) have studied the removal of manganese from water by precipitation. At a final pH of 8.5 (initial pH 5.5-9.0), limestone removed 95% of manganese, crushed brick 82%, gravel about 60% and the removal with no solid media was less than 15%. Their results indicated that rough solid media and the presence of carbonate are beneficial to the precipitation of manganese in water.

However, due to the limitations of active treatment, alternative passive treatments have been investigated. In passive systems the treatment is promoted by passing the effluent through stationary devices (wetlands, channels and drains) where the neutralizing agents are placed (abiotic) or where the biochemical treatment is performed (biotic). Passive biological systems can be performed in wetlands classified as aerobic or anaerobic (Johnson and Hallberg, 2005).

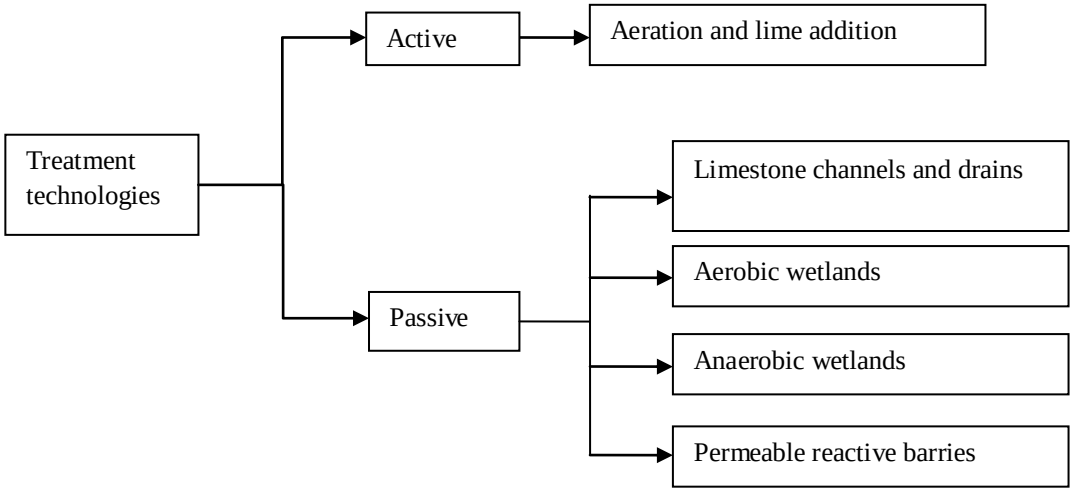

Figure 3.1: Active and passive treatment technologies for AMD remediation (Adapted from Johnson and Hallberg, 2005).

A number of researchers have reported experiments and treatment systems in which Mn bearing solutions flow through limestone beds. Experiments comparing a limestone bed with a gravel bed (aluminosilicate rock) showed that the limestone bed was much more effective in removing manganese (Aziz and Smith, 1996).

The most common method using a limestone bed is the patented Vail and Riley system, also named the "Pyrolusite" System, in which a bed of limestone is inoculated with Mn-oxidizing bacteria. Effective Mn removal requires oxidizing well-aerated water, as well as prior removal of essentially all dissolved Fe and Al, and pH above about 6.5. Most of the Pyrolusite systems removed manganese from influent values of 6 to 30 mg L^{-1} to effluent levels between 0.5 to 1.5 mg L^{-1} for a period of 2 years or more, but several of the systems have failed because of plugging of the inlet area with silt, leaves, Fe and/or Al precipitates, grass and other materials (Rose *et al.*, 2003b).

Wetlands consist of a complex ecosystem represented by the interaction between terrestrial and aquatic systems that can be used to remediate AMD. Commonly known as biological filters, wetlands have emerged as a viable option for helping to solve a wide range of environmental and water quality problems. Research on utilization of wetlands for the treatment of AMD to remove contaminants has been carried out in the past decade. Heavy metals removal from AMD in wetlands is done by physical, chemical and various biological processes which involve sedimentation, settling, filtration, adsorption, precipitation, co-precipitation into insoluble compounds (Sheoran and Sheoran, 2006). Even though manganese readily precipitates, little oxidation of Mn(II) occurs in solutions below pH 8. In addition, biological oxidation of Mn(II) does not proceed rapidly in the presence of Fe(II), and thus it is not removed significantly in aerobic wetlands where the concentration of ferrous iron exceeds 1 mg L^{-1}. Manganese does not readily form an insoluble sulfide phase and thus it is not removed to a great extent in anaerobic wetlands, though it may precipitate in these systems as rhodocrosite ($MnCO_3$) (Hallberg and Johnson, 2005).

Permeable reactive barriers (PRBs) are being increasingly used to treat a wide range of polluted ground waters. Some have been installed to bioremediate AMD. The construction of PRBs involves digging of a trench or pit in the flow path of contaminated groundwater, filling the void with reactive materials (a mixture of organic solids and possibly limestone gravel) that are sufficiently permeable to allow free flow of the groundwater, and landscaping of the disturbed surface. Reductive microbiological processes within the PRB generate alkalinity (which is further enhanced by dissolution of limestone and/or other basic minerals) and remove metals as sulfides, hydroxides, and carbonates (Johnson and Hallberg, 2005).

As manganese is generally not efficiently removed by current passive technologies applied to remediate mine water, alternative approaches are needed (Hallberg and Johnson, 2005).

Another possibility to remove manganese includes their adsorption onto active sites such as those found on algae and/or organic and inorganic compounds (Soto *et al*., 2005). The use of adsorbent/ion exchange resin is a promising alternative method for the removal of metals in dilute solution (Laus *et al*., 2005).

3.3.1. Manganese removal by adsorption/ion exchange

Adsorption processes may be used to remove metals, as soluble ions or complexes, from water solutions. It represents an interesting alternative to be used when it is desired to get very low residual concentrations of contaminants in water (Soto *et al*., 2005). In the case of manganese removal by adsorption/ion exchange, just a few works have been reported (Korn *et al*., 2004; Soto *et al*., 2005; Bosco *et al*., 2005, Mohan and Chander, 2006b).

Korn *et al*. (2004) evaluated the separation and concentration of trace manganese, copper and zinc from saline waters using adsorption of these metal ions onto the resins Dowex 1X8-50 and Amberlite XAD-7 in the range of pH between 3.0 and 10.0. It was observed that a maximum amount of Mn(II) removed was from the saline water at pH

9.0 for Amberlite XAD-7 and pH 8.0 for resin Dowex 1X8-50. The maximum loads obtained were 67 μg g^{-1} Dowex 1X8-50 and 1000 μg g^{-1} Amberlite XAD-7.

The removal of manganese present in aqueous solutions of concentration below 40 mg L^{-1} was investigated by Soto *et al*. (2005) using palygorskite (philossilicate) as an adsorbent in the range of pH between 4.5 and 8.5. The maximum loading of manganese (6.28 mg g^{-1}) occurred at pH 7.5 since, at pH 8.5, manganese precipitated, possibly as some kind of hydroxide.

Bosco *et al*. (2005) conducted studies on the ion exchange scolecite, a natural zeolite from Brazil, applied in the purification of water contaminated with heavy metals. The maximum retention of these metals occurred at pH around 6, and the decreasing order of adsorption of metals was Cr>Mn>Cd>Ni. The maximum retention of manganese was 75%.

Mohan and Chander (2006a) used lignite for the remediation of ferrous, ferric, and manganese ions in single, binary, ternary, and multicomponent systems from water/wastewaters. They showed that the sorption capacity increased with the increase in temperature in the case of Fe(II). The increase in temperature from 10 to 40ºC doubled the adsorption capacity from 24 to 46 mg g^{-1}. On the other hand, Mn(II) adsorption decreased with the increase in temperature. A decrease in temperature from 40 to 25ºC increased sorption capacity from 7.7 to 25 mg g^{-1}. The maximum adsorption capacities of the lignite were 46.46 (40ºC), 28.11 (10ºC), and 11.90 (25ºC) mg g^{-1} for Fe(II), Mn(II), and Fe(III), respectively. They also considered that an ion exchange process must be the predominant mechanism in the sorption of metals on lignite.

Aziz and Smith (1992) reported the removal of manganese from water using limestone, crushed brick and gravel. At a final pH value of 8.5, limestone removed 95% of manganese, crushed brick 82%, gravel about 60% and the removal for aeration and settlement with no solid media was less than 15%. But the results indicate that the presence of carbonates must have precipitated the manganese in water, which is not interesting for adsorption. It forces the system to control pH to prevent this unwanted precipitation.

Aziz and Smith (1996), in another study, developed a filtration technique using crushed dolomite to remove the manganese (1 mg L^{-1}) present in synthetic solutions at pH 7. According to these authors, dolomite was the most effective material for the removal of manganese. To optimize the use of dolomite as a filtering material, tests were conducted where the best removal occurred for particles with size of 500 mm and a flow rate of 10 mL min^{-1}. The authors suggest that the dolomite, having a low price and good adsorption of manganese, should be employed for water filtration systems.

Silva *et al.* (2010) evaluated limestone as an adsorbent for Mn removal. Batch experiments were carried out with synthetic solutions, at initial pH 5.5 and 8.3 g limestone L^{-1} and similarly, continuous tests were performed with 16.5 mg L^{-1} Mn^{2+} mine water, at initial pH 8.0 and 20.8 g limestone L^{-1}. Best results were achieved with calcite limestone and its fine grinding proved to be the most effective parameter for manganese removal. In either synthetic solutions or industrial effluents, the final manganese concentration was below 1 mg L^{-1}. A neutralization step to increase the effluent pH before efficient metal removal was necessary.

Robinson-Lora and Brennan (2010a) reported the role of chitin and chitin-associated proteins in the removal of manganese from AMD under abiotic and anaerobic conditions. The results showed that both types of biomolecules are capable to sorb manganese, however, the removal capacity of the chitinous materials significantly increases when chitin-associated proteins are present. At higher pH regimes, q_m values ranged from 0.165 (at pH 5.4) to 0.981 mg g^{-1} (at pH 8.7) for "pure" chitin and increased from 0.878 (at pH 5.2) to 5.437 mg g^{-1} (at pH 8.6) when both chitin and protein were present. Results clearly suggest that the chitin-associated proteins offer additional sorption sites for manganese.

Chitosan microspheres were shown by Laus *et al.* (2005) to be a promising material for remediation of acidity, iron and manganese removal from water contaminated by mining operation. Around 0.4 g of chitosan microspheres was necessary to remove nearly 90% of manganese (II). The results regarding the removal of manganese (II) are

interesting, since there are few alternatives for water recovery with this type of contamination.

3.4. Bone char

Bone char has been extensively used as an adsorbent for the decolorization of cane and beet sugar and to a lesser extent for the defluoridation of drinking water. After use, it is regenerated by washing and calcining so that the char can pass through many operating cycles before its activity has decreased to an unacceptably low level (Choy *et al*., 2004). Results for the removal of metal ions from wastewaters (Choy *et al*., 2004; Guedes *et al*., 2007; Pan *et al*., 2009; Ozawa *et al*., 2003; O'Connor and Weatherley, 1997) have been also reported.

Bone char is produced by the pyrolysis of crushed animal bones. After being ground to the appropriate particle size, the bone fragments are calcined at 800^{o}C under controlled conditions. X-ray diffraction reveals that bone char is a mixed adsorbent composed approximately of tricalcium phosphate (70-76 wt%), carbon content (9-11 wt%) and calcium carbonate (7-9 wt%) (Guedes *et al*., 2007). Structurally, calcium phosphate is in the hydroxyapatite form. The amorphous carbon fraction is distributed throughout the whole of the hydroxyapatite structure, but mostly exists as a highly active thin film over about 50% of the porous of hydroxyapatite surface (Choy *et al*., 2004).

Although production and use of bone char in large scale has been currently done in many countries, mainly for industrial sugar decolorization, the scientific literature on the preparation and use of bone char as an adsorbent is very small compared to the amount of literature on the other types of sorbents (Oliveira and Franca, 2008). Scientific publications on the application of bone char as adsorbent has aroused interest (Cheung *et al*., 2000; Cheung *et al*., 2001; Ko *et al*., 2000; Ko *et al*., 2004; Choy *et al*., 2004; Choy and McKay, 2005a,b; Ribeiro, 2011).

The sorption of metal ions copper, cadmium, and zinc onto bone char was demonstrated by Choy *et al*. (2004). Equilibrium studies have been analyzed using the Langmuir isotherm equation and the maximum sorption capacities for the metals were 45.1, 53.6,

and 33.0 mg g^{-1} bone char for copper, cadmium and zinc ions, respectively. Guedes *et al*. (2007) also studied the sorption of metal ions onto bone char and the maximum sorption capacities for the metals were 25.7, 27.0 and 25.3 mg g^{-1} bone char for copper, cadmium and zinc ions, respectively.

Pan *et al*. (2009) reported that swine bone char is effective in removing cobalt from solution. Batch kinetics studies showed that a rapid uptake occurred within the first 5 min. When the ratio of cobalt to bone char was greater than 0.3, nearby 1.0 mol of calcium was released as 1.0 mol of cobalt was adsorbed. The measurements of calcium concentrations in the solution containing the metal ions suggested that ion-exchange is the most significant mechanism for the removal of cobalt from the solution.

Hassan *et al*. (2008) used camel bone char for quantitative removal of Hg(II) from wastewater. The removal of mercury from 100 mL of 10 mg L^{-1} of Hg(II) was achieved by 0.03 g of camel bone charcoal at pH 2. The Langmuir adsorption capacity was 28.3 mg of Hg(II) per gram of the adsorbent.

Cheung *et al*. (2000) reported the sorption capacity of bone char for copper and zinc ions (47.7 and 34.7 mg g^{-1}, respectively) and concluded that bone char is a suitable sorbent for the two metal ions.

Cheung *et al*. (2001), in another study, evaluated the adsorption of cadmium ions onto bone char. Equilibrium tests were done to evaluate the sorption capacity of bone char for cadmium ions and experimental results showed it to be 64.1 mg g^{-1} at an equilibrium solution concentration of 337 mg L^{-1}. Since the sorption capacity is relatively high, it was concluded that bone char can be considered as a suitable sorbent for the adsorption of cadmium in wastewater treatment systems.

The removal of As(V) from aqueous solutions using bone char was studied by Chen *et al*. (2008). The adsorption was found to be strongly dependent on pH, dosage of adsorbent, and contact time. Bone char removed 99.18% of As(V) at the initial As(V) concentration of 0.5 mg L^{-1} and pH 10.

Ozawa *et al*. (2003) used fish bone hydroxyapatite for manganese removal from laboratory solution. The initial concentration of Mn(II) was 16 mg L^{-1} and 0.3 g of the bone powders was added to each 2 L of aqueous solution. After the mixture of powder and solution to be stirred for 2 hours and held for 6 days without stirring, the maximum adsorption capacity reached was 17 mg g^{-1}.

According to O'Connor and Weatherley (1997) the hydroxyapatite component of the bone char plays an important role in the adsorption of manganese, with adsorption occurring by ion exchange. Over 67% of manganese removals in twenty four hours for an initial concentration of 15 mg L^{-1} using bone char for manganese adsorption from potable water supplies.

Gonçalves (2006) studied the use of bone char in alkaline medium for manganese removal. 22% of manganese present in AMD effluent using 0.2 g of bone char and 200 mL of effluent for an initial concentration of 173 mg L^{-1}.

3.5. Adsorption

Adsorption can be described as mass transfer phenomena of solutes (adsorbate) from a fluid phase to a solid surface used as adsorbent. It is an operation that can solve or attenuate the problems of pollutants dissolved in liquid effluent and also those related to constituents in low concentrations in industrial processes, which need to be recovered due to their high added value (Gonçalves, 2006).

Adsorption is normally classified as physical or chemical process depending on the kind of interaction or strength existing between the adsorbent and the adsorbate. Physical adsorption occurs when weak interparticle bonds exist between the adsorbate and the adsorbent. Physical adsorption is easily reversible, in the majority of cases, what may lead to the adsorbent reutilization. Chemical adsorption, on the other hand, occurs when strong interparticle bonds are present between the adsorbate and the adsorbent. Chemisorption is deemed to be irreversible in the majority of cases (Reynolds and Richards, 1995).

3.5.1. Adsorption isotherms

The adsorption isotherm is, as well, an important tool to predict thermodynamic parameters. Several isotherm equations are available and the most common isotherms which are considered in many studies are the Langmuir and Freundlich isotherms.

3.5.1.1. Langmuir isotherm equation

The Langmuir adsorption isotherm, based on a theoretical model (Gibbs equation), assumes monolayer adsorption over an energetically and structurally homogeneous adsorbent surface. The saturation monolayer can be represented by the expression:

$$q_e = \frac{q_m b C_e}{1 + b C_e} \tag{3.5}$$

and a linear form:

$$\frac{1}{q_e} = \frac{1}{q_m} + \frac{1}{b q_m C_e} \tag{3.6}$$

in which q_e (mg g^{-1}) is the adsorption capacity by weight at equilibrium, q_m (mg g^{-1}) is the theoretical maximum adsorption capacity by weight, and b (L mg^{-1}) represents the Langmuir constant, while C_e (mg L^{-1}) is the concentration of adsorbate at equilibrium (Annadurai *et al*., 2008).

3.5.1.2. Freundlich isotherm equation

Freundlich proposed an empirical isotherm equation given by:

$$q_e = K_F C_e^{1/n} \tag{3.7}$$

or the linear form:

$$ln(q_e) = \frac{1}{n} ln(C_e) + ln(K_F) \tag{3.8}$$

in which K_F ($mg^{1-(1/n)}$ $L^{1/n}$ g^{-1}) represents the relative adsorption capacity and n is related to the intensity of adsorption, with values of n>1 indicating favorable adsorption. As the Freundlich isotherm equation is exponential, it can only be reasonably applied in the low to intermediate concentration ranges (Annadurai *et al*., 2008).

3.5.2. Adsorption kinetics

In adsorption systems, the mass transfer of solute or sorbate onto and within the sorbent particle directly affects the adsorption kinetics. In general, adsorption theory is based on the principle that four steps are involved in the process, any of which could be the rate-controlling step. The four steps are (Levenspiel, 2003):

- Transport of sorbate from the bulk of the solution to the boundary layer;
- Movement of sorbate across the external liquid film boundary layer to external surface sites;
- Migration of sorbate within the pores of the sorbent by intraparticle diffusion;
- Sorption of sorbate at internal surface sites.

There are, in the literature, several models proposed to fit the experimental data obtained by adsorption process. Among these, some are based on adsorption capacity of adsorbent material, which treats the data without considering, none of the steps involved in the adsorption process; the most used of these are the pseudo-first order and the pseudo-second order. However, there are also those that allow analyzing the mechanisms involved in the adsorption process, which may be related to the occurrence of a chemical reaction and/or mechanisms diffusion (Crini and Badot, 2008). In these cases, the most used are the diffusion in the film and intraparticle diffusion. In order to examine the mechanism controlling the adsorption processes, such as mass transfer and chemical reactions, several kinetic models are used to fit experimental data.

3.5.2.1. Pseudo-first-order equation

The pseudo-first-order kinetic equation or the so-called Lagergren equation has the following formulation:

$$\frac{dq_t}{dt} = k_1(q_e - q_t) \tag{3.9}$$

After definite integration by applying the initial conditions $q_t = 0$ at $t = 0$ and $q_t = q_t$ at $t = t$, equation (3.9) becomes:

$$log(q_e - q_t) = log(q_e) - \frac{k_1}{2.303}t \tag{3.10}$$

in which q_t is the amount of adsorbate adsorbed at time t, q_e is its value at equilibrium and k_1 (min^{-1}) is a constant of the pseudo-first-order adsorption. The equilibrium adsorption capacity q_e and the first-order constants k_1 can be determined experimentally from the slope and the intercept of plot of $\log(q_e - q_t)$ versus t. Generally, the pseudo-first-order equation fits the data when the rate-controlling step is the diffusion across the external liquid film boundary layer (Lagergren, 1898, *apud* Annadurai *et al*., 2008).

3.4.2.2. Pseudo-second-order equation

The pseudo-second-order equation based on adsorption equilibrium capacity may be expressed in the form:

$$\frac{dq_t}{dt} = k_2(q_e - q_t)^2 \tag{3.11}$$

Integrating equation (3.12) and applying the initial conditions described above:

$$\frac{t}{q_t} = \frac{1}{k_2(q_e)^2} + \frac{1}{q_e}t \tag{3.12}$$

in which k_2 (g mg^{-1} min^{-1}) is a constant of the pseudo-second-order adsorption. The equilibrium adsorption capacity q_e and the second-order constants k_2, can be determined experimentally from the slope and the intercept of plot t/q_t versus t. In general, the pseudo-second-order expression is used to describe chemisorption (Ho, 2006).

3.5.2.3. Intraparticle-diffusion model

Intraparticle diffusion has a significant role in many adsorption processes and assumes that diffusion of adsorbate occurs within the pore structure of the adsorbent. The intraparticle diffusion model can be described as:

$$q_t = K_p.t^{1/2} + C \tag{3.13}$$

where k_p (mg g^{-1} $min^{-0.5}$) is the intraparticle diffusion constant, evaluated as the slope of the curve q_t versus $t^{1/2}$ and *C* (mg g^{-1}) is the constant related to the boundary layer thickness. If the regression of q_t *versus* $t^{1/2}$ is linear and passes through the origin, then intraparticle diffusion is the sole rate-limiting step. However, if this line does not pass through the origin, this indicates some degree of control associated with the diffusion boundary layer. In this case, it can occur due to the fact that either (i) intraparticle diffusion is not the rate-limiting step of the process, or that (ii) beyond this step, another step in the adsorption mechanism also requires a time significant to occur, so together controlling the rate of adsorption process (Weber and Morris, 1963 *apud* Annadurai *et al*., 2008).

3.5.3. Fixed bed adsorption

Batch adsorption experiments are easily used in laboratory scale for the treatment of small volume of effluents, but it is less convenient to use on industrial scale, where large volumes of wastewater are continuously generated. Batch adsorption provides certain preliminary information such as the pH for maximum adsorption, maximum initial metal ion concentration, and particle size for optimum adsorption of metal ions, and approximate time for adsorption of metal ion as well as the adsorption capacity of the adsorbent. All these information are useful for packed bed studies.

In fixed bed adsorption, the solute concentration in the solid is initially zero. Feed solution is added into the fixed bed, giving the abrupt concentration profiles that move through the bed. The concentration in the solid is either zero or in equilibrium with the concentrated feed. In the stirred tanks, the situation is very different. Both solid and solution are stirred together. At very short time, the solution concentration is higher than

that in the solid. After a while, mass transfer increases the concentration in the solid and depletes that in solution. At long time, the solid reaches an equilibrium, but with the depleted solution. This equilibrium concentration is much less than that with the feed solution. Thus the stirred tank has a much less effective separation than the fixed bed (Cussler, 1997).

In fixed bed adsorption, the concentration in the liquid phase and in the solid phase change with time as well as with position in the bed. At first, most of the mass transfer takes place near the inlet of the bed, where the fluid first contact the adsorbent. With time, the mass transfer zone moves down the bed. Although the packed bed systems can be fed with flows upward or downward, it is important to note that flows upward under high flow may fluidize the bed, causing friction between the particles. In excess, this can result in reduction of average particle size of the bed and therefore the loss of the material adsorbent (McCabe *et al*., 2005).

The design and theory of fixed bed adsorption systems focuses on establishing the shape of the breakthrough curve and its velocity through the bed. Breakthrough curves *versus* time plots can be easily plotted because this is the way in which data are most commonly attained. However, it can sometimes gain more insight into the behavior of these beds by plotting breakthrough curves versus the treated volume or versus the number of bed volumes. Plotting a breakthrough curve versus treated volume is useful to compare different adsorbents. For a nonadsorbing solute, the breakthrough occurs when the eluted volume equals the void volume in the fixed bed. For a strongly adsorbing solute, the breakthrough occurs when the treated volume is much greater than the void volume in the fixed bed. As a result, the adsorption data are not plotted versus time or eluted volume, but versus the number of bed volumes, that is the eluted volume divided by the volume of bed's voids (Cussler, 1997).

Measuring the concentration of adsorbate in the stream leaving the column and constructing a graph with these values in function of number of bed volumes or time, results in the breakthrough curve as shown in Figure 3.2 (McCabe *et al*., 2005).

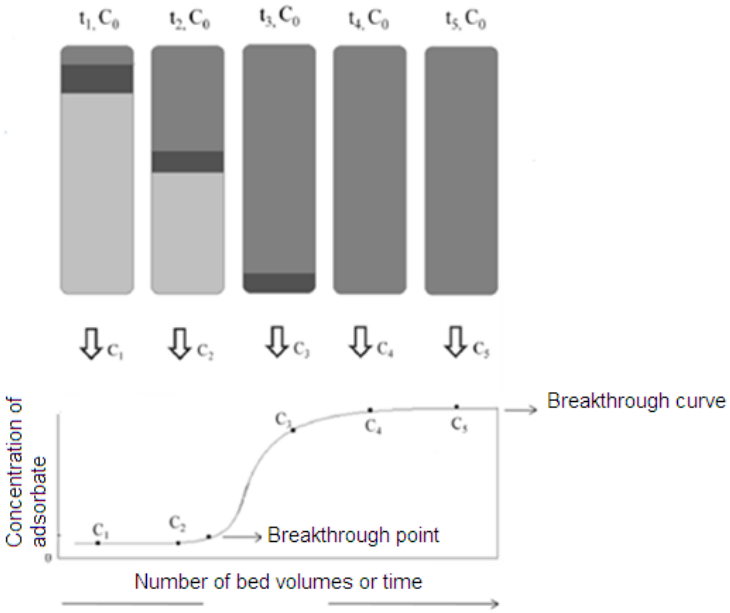

Figure 3.2: Breakthrough curve for adsorption in a fixed bed (Adapted from Reynolds and Richards, 1995).

Figure 3.2 describes a process which presents a fixed bed column with height h, fed with a solution of concentration C_0, pumped at a continuous flow rate Q. The breakthrough point represents the point where the adsorbate starts to be detected at the outlet of the column, so it is normally used to determine the capacity of a given column.

3.5.3.1. Adsorption kinetics in fixed bed systems

Although the fixed bed adsorption follows the same steps of the batch adsorption process, the mass transfer phenomena is not necessarily the same. Therefore, data obtained in experimental systems in fixed bed adsorption are evaluated and described by different models.

The Thomas model is commonly used in the modeling of fixed bed breakthrough curves in environmental sorption research (Unuabonah *et al.*, 2010). It is widely used for the design of activated carbon adsorbers due to theirs simplicity. The Thomas model assumes a Langmuir (favorable) isotherm (Chu, 2010).

The expression by Thomas for an adsorption column is given as follows:

$$\frac{C_t}{C_0} = \frac{1}{1+\exp\left(k_T\left(\frac{q_0 M}{Q} - C_0 t\right)\right)} \tag{3.14}$$

The linearized form of Thomas model can be expressed as follows:

$$\ln\left(\frac{C_0}{C_t} - 1\right) = \frac{k_T q_0 M}{Q} - k_T C_0 t \tag{3.15}$$

in which k_T (L mg^{-1} min^{-1}) is the Thomas rate constant, q_0 is the sorption capacity of the adsorbent per unit mass (mg g^{-1}), M is the mass of adsorbent (g) and Q is the flow rate (L min^{-1}).

The kinetic coefficient k_T and the adsorption capacity q_0 can be obtained from the plot of $\ln\left(\frac{C_0}{C_t} - 1\right)$ against time (t) at a given flow rate using linear regression (Cavas *et al*., 2011).

3.6. Desorption

Adsorption studies can be complemented with desorption ones. Such studies aims to recover the metal retained and reuse the adsorbent in subsequent loading and unloading cycles. When the adsorbent becomes exhausted or when the effluent from the adsorbent bed reaches the maximum allowable discharge level, the recovery of the adsorbent material becomes necessary. Regeneration of spent adsorbent columns is quite an important process in wastewater treatment. In this process, 10–20% of the adsorbent is usually lost by attrition during each cycle and the recovery of the adsorbate is also not possible (Mohan and Chander, 2006b).

Desorption studies of lignite loaded with manganese were performed by Mohan and Chander (2006b). To simulate industrial conditions for acid mine wastewater treatment, all tests were carried out using single and multi-columns setup in down flow mode. Desorption of metal ions in three column systems was conducted with 0.1 mol L^{-1} HNO_3 and showed that the recovery of the metal ions was almost 100%.

Desorption experiments with bone char loaded with Zn were carried out by Guedes *et al*. (2007). The first desorption test was carried out with 10 g L^{-1} of bone char in distilled water at pH 5.4. The second desorption experiment was carried out with sulfuric acid solution (0.01 mol L^{-1}) at the same conditions as for distilled water. It was observed that desorption with distilled water was not effective but in the case of desorption carried out with the sulfuric acid solution, the levels of desorption was 40%.

3.7. References

ANNADURAI, G.; LING, L.Y.; LEE, J.F. Adsorption of reactive dye from solution by chitosan: isotherm, kinetic and thermodynamic analysis. *Journal of Hazardous Materials*, v. 152, p. 337-346, 2008.

AZIZ, H.A.; SMITH, P.G. Removal of manganese from water using crushed dolomite filtration technique. *Water Research*, v. 30, p. 489-492, 1996.

AZIZ, H.A.; SMITH, P.G. The influence of pH and course media on manganese precipitation from water. *Water Research*, v. 26, p. 853-855, 1992.

BAMFORTH, S.M.; MANNING, D.A.C.; SINGLETON, I.; YOUNGER, P.L.; JOHNSON, K.L. Manganese removal from mine waters – investigating the occurrence and importance of manganese carbonates. *Applied Geochemistry*, v. 21, p. 1274-1287, 2006.

BOSCO, S.M.D.; JIMENEZ, R.S.; CARVALHO, W.A. Removal of toxic metals from wastewater by Brazilian natural scolecite. *Journal of Colloid and Interface Science*, v. 281, p. 424-431, 2005.

CAVAS, L.; KARABAYA, Z.; ALYURUKA, H.; DOGAN, H.; DEMIR, G.K. Thomas and artificial neural network models for the fixed-bed adsorption of methylene blue by a beach waste Posidonia oceanica (L.) dead leaves. *Chemical Engineering Journal*, v. 171, p. 557-562, 2011.

CHEN, Y.-N.; CHAI, L.-Y.; SHU, Y.-D. Study of arsenic(V) adsorption on bone char from aqueous solution. *Journal of Hazardous Materials*, v. 160, p. 168-172, 2008.

CHEUNG, C.W.; PORTER, J.F.; McKAY, G. Sorption kinetic analysis for the removal of cadmium ions from effluents using bone char, *Water Research*, v. 35, p. 605-612, 2001.

CHEUNG, C.W.; PORTER, J.F.; McKAY, G. Sorption kinetics for the removal of copper and zinc from effluents using bone char. *Separation and Purification Technology*, v. 19, p. 55-64, 2000.

CHOY, K.K.H.; McKAY, G. Sorption of cadmium, copper, and zinc ions onto bone char using Crank diffusion model. *Chemosphere*, v. 60, p. 1141-1150, 2005a.

CHOY, K.K.H.; McKAY, G. Sorption of metal ions from aqueous solution using bone char, *Environment International*, v. 31, p. 845-854, 2005b.

CHOY, K.K.H.; BARFORD, J.P.; McKAY, G. Production of activated carbon from bamboo scaffolding waste-process design, evaluation and sensitivity analysis, *Chemical Engineering Journal*, v. 109, p. 147-165, 2005.

CHOY, K.K.H.; KO, D.C.K.; CHEUNG, C.W.; PORTER, J.F.; McKAY, G. Film and intraparticle mass transfer during the adsorption of metal ions onto bone char. *Journal of Colloid and Interface Science*, v. 271, p. 284-295, 2004.

CHU, K.H. Fixed bed sorption: Setting the record straight on the Bohart–Adams and Thomas models. *Journal of Hazardous Materials*, v. 177, p. 1006-1012, 2010.

CONSELHO NACIONAL DO MEIO AMBIENTE. Resolução CONAMA n.º 357/2005: Classificação dos corpos de água e diretrizes ambientais para o seu enquadramento, bem como estabelece as condições e padrões de lançamento de efluentes. Brasília, 2005. Disponível na Web em: http://www.mma.gov.br/port/conama/index.cfm.

CRINI, G., BADOT, P. Application of chitosan, a natural aminoplysaccharide, for dye removal from aqueous solutions by adsorption processes using batch studies: a review of recent literature. *Progress in Polymer Science*, v. 33, p. 399-447, 2008.

CUSSLER, E.L. Diffusion: Mass Transfer in Fluid Systems. 2nd edition. Cambridge University Press, p. 312-314, 1997.

GONÇALVES, C.R. Remoção de manganês e recuperação de urânio presentes em águas ácidas de mina. Belo Horizonte, 2006. Dissertação (Mestrado) - Centro de Desenvolvimento da Tecnologia Nuclear.

GUEDES, T.S.; MANSUR, M.B.; ROCHA, S.D.F. A perspective of bone char use in the treatment of industrial liquid effluents containing heavy metals. In: XXI ENTMME, Ouro Preto - MG, 2007.

HALLBERG, K.B.; JOHNSON, D.B. Biological manganese removal from acid mine drainage in constructed wetlands and prototype reactors. *Science of the Total Environment*, v. 338, p. 115-124, 2005.

HASSAN, S.S.M; AWWAD, N.S.; ABOTERIKA, A.H.A. Removal of mercury(II) from wastewater using camel bone charcoal. *Journal of Hazardous Materials*, v. 154, p. 992-997, 2008.

HO, Y.S. Review of second-order models for adsorption systems. *Journal of Hazardous Materials*, B136, p. 681-689, 2006.

JOHNSON, D.B.; HALLBERG, K.B. Acid mine drainage remediation options: a review. *Science of the Total Environment*, v. 338, p. 3-14, 2005.

KO, D.C.K.; PORTER, J.F.; McKAY, G. Optimised correlations for the fixed-bed adsorption of metal ions on bone char. *Chemical Engineering Science*, v. 55, p. 5819-5829, 2000.

KO, D.C.K.; CHEUNG, C.W.; CHOY, K.K.H.; PORTER, J.F.; McKAY, G. Sorption equilibria of metal ions on bone char, *Chemosphere*, v. 54, p. 273-281, 2004.

KORN, M.G.A., SANTOS JR., A.F., JAEGER, H.V., SILVA, N.M.S., COSTA, A.C.S., 2004. Cooper, zinc and manganese determination in saline samples employing FAAS after separation and preconcentration on Amberlite XAD-7 and Dowex 1X-8 loaded with alizarin Red. *Journal of Brazilian Chemical Society*, 15(2), 212-218.

LANGERGREN. Zur theorie der sogenannten adsorption geloster stoffe, Kungliga Svenska Ventenskapsaka demiens, Handlingar 24, p. 1–39, 1898 apud ANNADURAI, G.; LING, L.Y.; LEE, J.F. Adsorption of reactive dye from solution by chitosan: isotherm, kinetic and thermodynamic analysis. *Journal of Hazardous Materials*, v. 152, p. 337-346, 2008.

LAUS, R.; LARANJEIRA, M.C.M.; MARTINS, A.O.; FÁVERE, V.T. Microesferas de quitosana reticuladas com tripolifosfato utilizadas para remoção da acidez, ferro(III) e manganês(II) de águas contaminadas pela mineração de carvão. *Quimica Nova*, v. 29, nº 1, p. 34-39, 2006.

LEVENSPIEL, O. Engenharia das reações químicas. Tradução da 3ª edição. São Paulo: Editora Blucher, 2003. p. 480-497.

LIND, C.J.; HEM, J.D. Manganese minerals and associated fine particulates in the streambed of Pinal Creek, Arizona, USA: a mining-related acid drainage problem. *Applied Geochemistry*, v. 8, p. 67-80, 1993.

LIU, Y.; LIU, Y.J. Biosorption isotherms, Kinetics and thermodynamics. *Separation and purification Technology*, v. 61, p. 229-242, 2008.

McCABE, W.L.; SMITH, J.C.; HARRIOTT, P. Unit operations of chemical engineering: Chemical Engineering Series. 7th edition. McGraw-Hill´s Science, p. 836-847, 2005.

MOHAN, D.; CHANDER, S. Single, binary, and multicomponent sorption of iron and manganese on lignite. *Journal of Colloid and Interface Science*, v. 299, p. 76-87, 2006a.

MOHAN, D.; CHANDER, S. Removal and recovery of metal ions from acid mine drainage using lignite - A low cost sorbent. *Journal of Hazardous Materials*, v. B137, p. 1545-1553, 2006b.

NASCIMENTO, M.R.L. Remoção e recuperaçâo de urânio de águas ácidas de mina por resina de troca iônica. São Carlos, 1998. Dissertação (Mestrado) - Universidade Federal de São Carlos.

O'CONNOR, J.M. AND WEATHERLEY, L.R. An investigation into the mechanism of adsorption of humic substances and trace metal compounds from potable water supplies. *Global Environmental Biotechnology*, p. 91-106, 1997.

OLIVEIRA, L.S.; FRANCA, A.S. Low-cost adsorbents from agri-food wastes. In: Food Science and Technology: New Research, Nova Science Publishers, chapter 3, 2008.

OZAWA, M.; SATAKE, K.; SUZUKI, S. Removal of aqueous manganese using fish bone hydroxyapatite. *Journal of materials science letters*, v.22, p.1363 – 1364, 2003.

PAN, X.; WANG, J.; ZHANG, D. Sorption of cobalt to bone char: Kinetics, competitive sorption and mechanism. *Desalination*, v. 249, p. 609-614, 2009.

REYNOLDS, T.D.; RICHARDS, P.A. Unit operations and processes in environmental engineering. 2ª Edição. Boston: PWS Publishing Company, p. 350-409, 1995.

RIBEIRO, M.V. Uso de Carvão de Osso Bovino na Defluoretação de Água para Uso em Abastecimento Público. Belo Horizonte, 2011. Dissertação (Mestrado) - Universidade Federal de Minas Gerais.

ROBINSON-LORA, M.A.; BRENNAN, R.A. Biosorption of manganese onto chitin and associated proteins during the treatment of mine impacted water. *Chemical Engineering Journal*. v. 162, p. 565-572, 2010a.

ROBINSON-LORA, M.A.; BRENNAN, R.A. Chitin complex for the remediation of mine impacted water: geochemistry of metal removal and comparison with other common substrates, *Applied Geochemistry*, v. 25, p. 336-344, 2010b.

ROBINSON-LORA, M.A.; BRENNAN, R.A. Efficient metal removal and neutralization of acid mine drainage by crab-shell chitin under batch and continuous-flow conditions. *Bioresource Technology*, v.100, p. 5063-5071, 2009.

ROSE, A.W.; MEANS, B.; SHAH, P.J. Methods for passive removal of manganese from acid mine drainage. In: 2003 West Virginia Surface Mine Drainage Task Force Symposium, Morgantown, WV, p. 11, 2003a.

ROSE, A.W.; SHAH, P.J.; MEANS, B. Case studies of limestone-bed passive systems for manganese removal from acid mine drainage. In: National Meeting of the American Society of Mining and Reclamation and the 9th Billings Land Reclamation Symposium, Billings MT, p. 1058-1078, 2003b.

SHEORAN, A.S.; SHEORAN, V. Heavy metal removal mechanism of acid mine drainage in wetlands: A critical review. *Minerals Engineering*, v.19, p. 105–116, 2006.

SILVA, A.M.; CRUZ, F.L.S.; LIMA, R.M.F.; TEIXEIRA, M.C.; LEÃO, V.A. Manganese and limestone interactions during mine water treatment. *Journal of Hazardous Materials*, v. 181, p. 514-520, 2010.

SOTO, O.A.J.; TOREM, M.L.; TRINDADE, R.B.E. Palygorskite as a sorbent in the removal of manganese(II) from water mine effluents. In: XIII INTERNATIONAL CONFERENCE ON HEAVY METALS IN THE ENVIRONMENT, Rio de Janeiro - RJ, 2005.

UNUABONAH, E.I.; OLU-OWOLABI, B.I.; FASUYI, E.I.; ADEBOWALE, K.O. Modeling of fixed-bed column studies for the adsorption of cadmium onto novel polymer–clay composite adsorbent. *Journal of Hazardous Materials*, v. 179, p. 415-423, 2010.

VAIL, W.J.; RILEY, R.K. The Pyrolusite Process: A bioremediation process for the abatement of acid mine drainage. *Green Lands*, v. 30 (4), p. 40-46, 2000 *apud* ROSE, A.W.; SHAH, P.J.; MEANS, B. Case studies of limestone-bed passive systems for manganese removal from acid mine drainage. In: National Meeting of the American Society of Mining and Reclamation and the 9th Billings Land Reclamation Symposium, Billings MT, p. 1058-1078, 2003b.

WEBER, W.J.; MORRIS, J.C. Kinetic of adsorption carbon solution, *Journal Sanitary Engineering Divisor*, American Society Civil Engineers v. 89, p. 31-59, 1963 *apud* ANNADURAI, G.; LING, L.Y.; LEE, J.F. Adsorption of reactive dye from solution by

chitosan: isotherm, kinetic and thermodynamic analysis. *Journal of Hazardous Materials*, v. 152, p. 337-346, 2008.

4. BATCH REMOVAL OF MANGANESE FROM ACID MINE DRAINAGE USING BONE CHAR

Dalila Chaves Sicupira[a], Thiago Tolentino Silva[a], Versiane Albis Leão[b] and Marcelo Borges Mansur[a,*]

[a] Departamento de Engenharia Metalúrgica e de Materiais, Universidade Federal de Minas Gerais

Av. Antônio Carlos, 6627, Campus Pampulha, 31270-901, Belo Horizonte, MG, Brazil

Tel.: +55 (31) 3409-1811; Fax: +55 (31) 3409-1716

E-mail: marcelo.mansur@demet.ufmg.br

* Corresponding author

[b] Departamento de Engenharia Metalúrgica e de Materiais, Universidade Federal de Ouro Preto

Campus Universitário, Morro do Cruzeiro, 35400-000, Ouro Preto, MG, Brasil

Abstract

Batch kinetics and equilibrium of manganese removal from acid mine drainage (AMD) have been investigated in this study. Equilibrium tests revealed that Langmuir based maximum manganese uptake capacity was 22 mg g^{-1} for AMD effluent and 20 mg g^{-1} for laboratory solution. Manganese kinetics onto bone char was best described by a pseudo-second order model. Manganese removal was mainly influenced by operating variables solid/liquid ratio and pH of the aqueous phase. In fact, manganese removal was favored at nearly neutral pH values. The effect of particle size and temperature was found to be not significant for the operating range investigated. The mechanism for the removal of manganese with bone char was evaluated. It has been found that intraparticle diffusion is the main rate-limiting step for manganese sorption systems but additional contribution from boundary layer diffusion might also affect removal when bone char particles of smaller sizes are used. The final concentration of fluoride and others metals present in the AMD effluent was in agreement with the limit concentration established by Brazilian legislation (CONAMA, 2005). The study revealed that bone char is a suitable material to be used for the removal of manganese from AMD effluents.

Key-words: manganese; bone char; acid mine drainage; adsorption.

4.1. Introduction

Given its dynamics and persistence, acid mine drainage (AMD) is one of the most serious environmental problems of the mining industry. Such phenomenon occurs when pyrite and/or other sulfide minerals are oxidized due to its exposure to oxygen and water, thus producing sulfuric acid that might dissolve metals species resulting in contamination of the environment (Nascimento, 1998). The main sources of AMD are open or underground pit mine, waste rock piles, tailings storage and ore stockpiles. The raise in the concentration of metal ions in the water due to AMD is an important source of contamination of watercourses, especially when ions can be spread to the food chain. Aiming to minimize the severity of such impacts, environmental protection laws require appropriate plans for mine closure as an attempt to increase the cycle life of closed mines including steps of decommissioning and recovery of degraded areas (Gonçalves, 2006).

In Brazil, AMD has been highlighted in coalfields in the south of the country and also in the Industrial Mining Complex of Poços de Caldas (Indústrias Nucleares do Brasil – INB), in the state of Minas Gerais. AMD generated in this last region contains radionuclides (uranium, thorium, radium, and others) and species like manganese, zinc, fluoride and iron at levels of concentration above those allowed by Brazilian legislation for direct discharge (Gonçalves, 2006; CONAMA, 2005). The current treatment of such acid water consists of metals precipitation with lime followed by pH correction. Most of metal species are precipitated but manganese ions removal from AMD is notoriously difficult to occur due to their complex chemistry in aqueous systems (Bamforth *et al.*, 2006; Robinson-Lora and Brennan, 2010). For complete precipitation of manganese, the pH must be raised to around 11; and it involves a significant consumption of lime, around 350 tons per month (Gonçalves, 2006). In addition, after manganese removal, the pH must be neutralized for discharge so such treatment is costly, generates large volumes of sludges and requires the consumption of huge quantities of reagents to be effective. Therefore, new technologies to treat AMD effluents containing manganese are urged.

The adsorption of metal species has been investigated using various alternative materials (Korn *et al.*, 2004; Bosco *et al.*, 2005; Soto *et al.*, 2005) but relatively little

attention has been directed to the manganese removal from AMD solutions. Adsorption has proven to be a particularly interesting technique in hydrometallurgical applications. It allows the recovery of ions from very dilute solutions and it has also the ability to process large volumes of solutions when other separating methods seem unfavorable.

Bone char has been successfully applied for the removal of various metal species such as copper, zinc, cadmium, arsenic, mercury, etc (Cheung *et al*., 2000; Choy *et al*., 2004; Chen *et al*., 2008; Hassan *et al*., 2008; Pan *et al*., 2009), however the use of bone char in the manganese removal has little information until date (O'Connor and Weatherley, 1997, Ozawa *et al*., 2003 and Gonçalves, 2006). As bone char consists basically of hydroxyapatite ($Ca_{10}(PO_4)_6(OH)_2$) and calcite ($CaCO_3$), its use could not only remove manganese but also raise the pH of the effluent due to the dissolution of the calcite, thus contributing to reduce the lime consumption currently used in the treatment of AMD solutions containing manganese.

In the view of the aforementioned, the aim of this work is to evaluate the feasibility of using bone char in the treatment of AMD effluents containing manganese. Batch equilibrium and kinetics tests were carried out using AMD effluents and laboratory solutions containing manganese at typical concentrations for comparative analysis.

4.2. Experimental

4.2.1. Reagents and instrumentation

AMD effluent generated by the industrial mining complex of Poços de Caldas (Indústrias Nucleares do Brasil – INB) and bone char supplied by Bone Char do Brasil Ltda were used in the present study. A laboratory solution containing 100 mg L^{-1} of manganese was also prepared using chemicals of analytical reagent grade dissolved in distilled water.

A mechanical shaker (Nova Ética 109) was used for agitating the sample solutions with bone char. Atomic emission spectrometer with inductively coupled plasma (ICP-AES Perkin Elmer OPTIMA 7300DV) was used for assessing the concentration of

manganese in the aqueous solutions. Sulfate and fluoride analysis were performed using a DX500 Dionex ion chromatograph. The pH measurements were carried out using a pH meter (Quimis). A scanning electron microscopy (SEM, JEOL JSM 5410) with X-ray energy dispersive spectrometry (EDS, NORAN VOYAGER 3.4.1) was employed to analyze the surface morphology and to obtain the elemental composition of the bone char. The solid was also analyzed by XRD (X-Ray Diffraction, using a PANalytical X'Pert APD diffractometer) and FTIR (Fourier Transform Infra-Red, using a Perkin Elmer Paragon 1000 spectrometer). In addition, surface area, total pore volume and average pore diameter were assessed by measuring multipoint N_2 isotherms in a BET Quantachrome model Autosorb 1C.

4.2.2. Manganese removal studies

4.2.2.1. Batch sorption kinetics

Kinetics tests were conducted with 400 mL of laboratory solution or effluent at room temperature and samples of aqueous solutions was collected with time. The solutions were placed with 2 g of bone char (solid/liquid ratio = 2/400 g mL^{-1}) and the mixture was magnetically stirred for 48 hours at a rotation speed of 150 min^{-1}, keeping constant pH due to the buffer effect from the calcite dissolution. Samples of the aqueous solutions (1 mL) were collected at fixed contact times, diluted, filtered and acidified using HNO_3 before being analyzed by ICP-AES. The influence of the solid/liquid ratio on the sorption kinetics of manganese was studied using different amounts of bone char, i.e., 1 and 3 g (solid/liquid ratio 1/400 and 3/400 g mL^{-1}, respectively). Kinetics sorption studies were also carried out using bone char samples at different particle size (417-833 µm, 104-147 µm and <53 µm) to determine the effect of particle sizes.

4.2.2.2. Batch sorption isotherms

In these experiments, a series of dilutions were prepared at concentration from 10 to 100 mg L^{-1} from the original effluent and laboratory solution. Aliquots of 100 mL of each dilution were placed into erlenmeyer flasks. The pH of effluent was first adjusted to 5.0 or 6.5 using $Ca(OH)_2$ solution (30%) in order to precipitate other metals and filtered. No pH adjustment was done to the laboratory solutions (initial pH = 5.7). In each flask,

250mg of bone char was added and the mixtures were shaken at 150 rpm and room temperature (25ºC) using a mechanical shaker for 48 hours. The effect of the following operating variables was investigated: initial pH of effluent (5.0 and 6.5) and temperature (10, 25 and 40ºC). After agitation, the pulp was filtered and the filtrate analyzed by ICP-AES to assess the metal concentration.

4.3. Results and discussion

4.3.1. Characterization analysis

4.3.1.1. Characterization of the bone char

The bone char has a real density of 2.9 g cm^{-3}. Its pore diameter includes mesopores. Table 1 shows the pore distribution for the particle size range studied. As a consequence of its highly porous nature (total pore volume 0.275 cm^3 g^{-1}), bone char shows a relative high surface area of 93 m^2 g^{-1}.

Table IV.1: Pore distribution for the particle size range studied.

Pore sizes (Å)	Pore distribution for 417-833 µm (%)	Pore distribution for <53 µm (%)
< 20	0.01	0.00
20-50	13.49	5.28
50-80	21.52	16.96
80-110	21.41	15.87
110-140	21.12	12.35
140-170	7.37	8.66
170-200	4.70	12.28
200-400	10.38	28.61

On the regard of composition, bone char contains both organic and inorganic compounds. According to the XRD analysis of the bone char (Figure 4.1), the main

phases presents are hydroxyapatite ($Ca_{10}(PO_4)_6(OH)_2$) and calcite ($CaCO_3$). The presence of such species is corroborated by FTIR spectrum analysis. Their characteristic vibrational bands are shown in Figure 4.2 (hydroxyl group at 3420 and 1630 cm^{-1}, phosphate group at 1035, 603 and 565 cm^{-1} and the carbonate group at 1457 cm^{-1}).

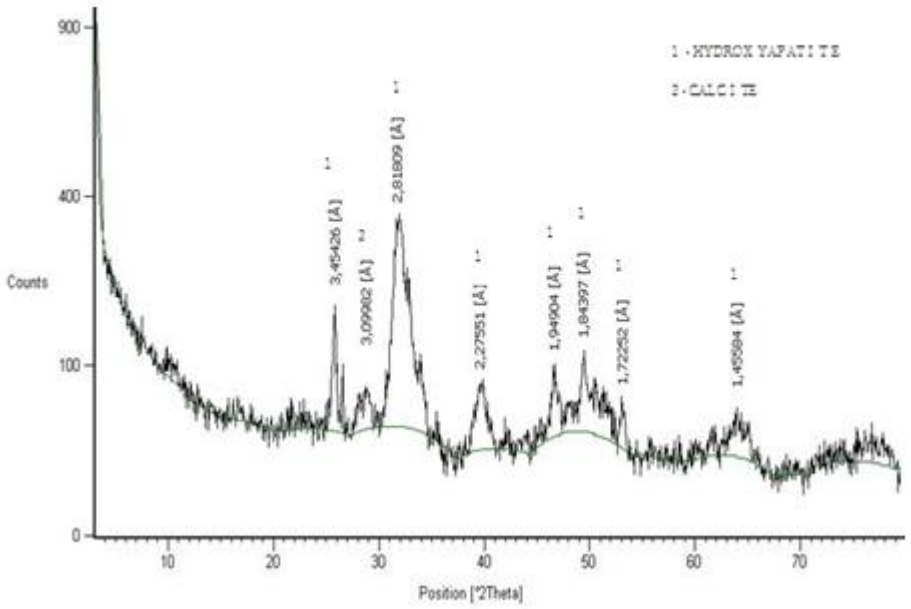

Figure 1.1: X-ray pattern of bone char.

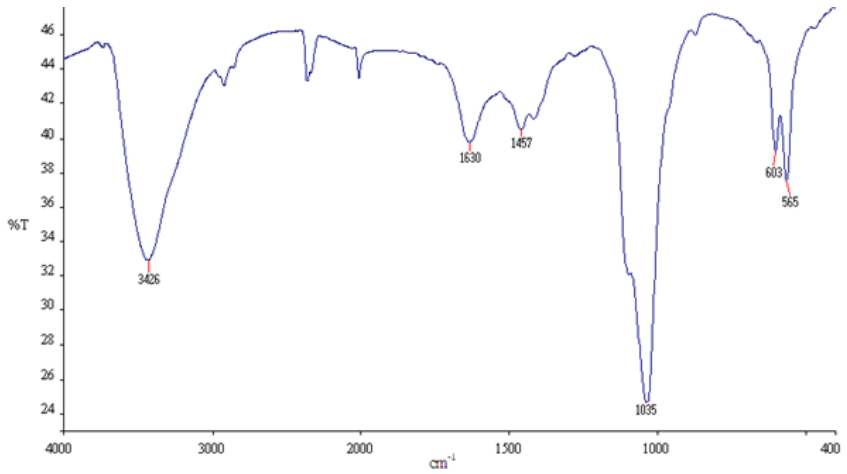

Figure 4.2: FTIR spectra of bone char using KBr discs

The morphology and the chemical composition of the bone char assessed by SEM-EDS before the contact with the AMD effluent, figures 4.3a and 4.3b, show a significant

presence of calcium and phosphorus, as expected. After the adsorption process (Figure 4.3c and 4.3d), a decrease in the relative Ca/P ratio was observed due to the dissolution of calcite. It was verified also the presence of manganese and others species (F, S, La, Ce), thus suggesting that such elements are present on the surface of the loaded bone char possibly due to some adsorptive and/or precipitating process.

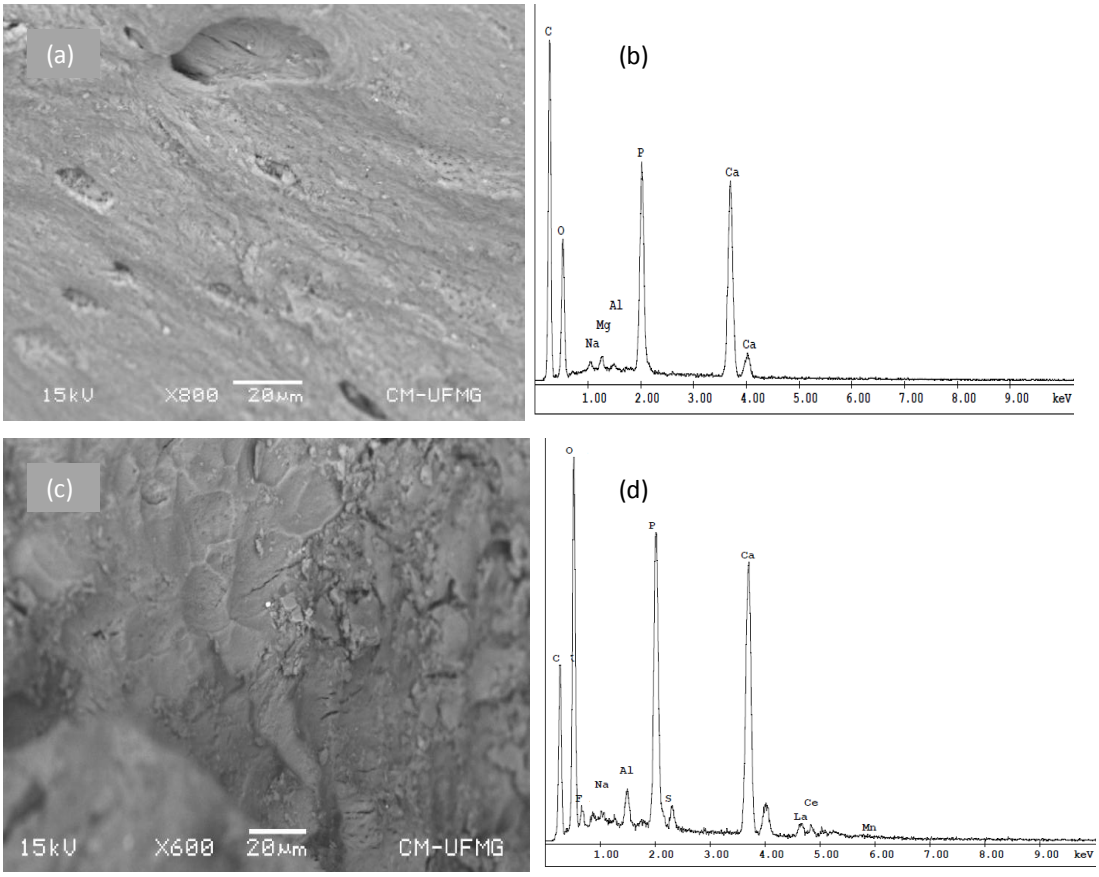

Figure 4.3: Morphology and chemical composition of bone char by SEM-EDS: (a, b) bone char as received, and (c, d) bone char after contact with AMD effluent.

4.3.1.2. Characterization of the AMD effluent

The AMD effluent used in this study was collected nearby the uranium mine of INB which is located in Poços de Caldas, Brazil. The composition of the effluent before and after precipitation with $Ca(OH)_2$ and the limit of resolution CONAMA 357 (Brazilian standard for effluent discharge) is shown in Table IV.2. It can be seen that manganese concentration in the AMD exceeds the maximum value of the Brazilian legislation. The same occurs to zinc and acidity, so treatment of effluent is mandatory. On the other

hand, the concentration of iron was found to be acceptable for discharge. After the precipitation with $Ca(OH)_2$, it can be seen that manganese concentration is still not in agreement with the Brazilian legislation, but the concentration of the others elements present in the AMD effluent are in agreement with it, except fluoride.

Table IV.2: Chemical characterization of the AMD effluent.

Parameters	Concentration ($mg\ L^{-1}$)	Concentration after precipitation ($mg\ L^{-1}$)	CONAMA 357 ($mg\ L^{-1}$)
U	6.8	<0.3	-
Mn	107.5	89.5	1.0
Ca	104.9	428	-
Mg	7.6	7.4	-
Al	164.2	28.5	-
Zn	17.7	4.0	5.0
Fe	<0.01	<0.01	15.0
F^-	99.0	38.0	10.0
SO_4^{2-}	1349	1335	-
pH*	2.97	5.64	6 to 9

* All parameters are expressed in $mg\ L^{-1}$, except pH.

- Permissible level not defined by the Brazilian legislation.

4.3.2. Batch sorption kinetics

The kinetic equation of pseudo-first order was found to be not adequate to fit the kinetics data for manganese removal ($R^2 \leq 0.71$ for all cases); in fact, a non-linear behavior over the time was obtained indicating that more than one mechanism is involved in the adsorption process. On the other hand, the kinetic equation of pseudo-second order fitted experimental data satisfactorily ($R^2 \geq 0.98$ for all cases). The linearized pseudo-second order equation is expressed as:

$$\frac{t}{q_t} = \frac{1}{k_2 q_e^2} + \frac{t}{q_e} \quad (4.1)$$

in which q_t (mg g^{-1}) is the amount of manganese adsorbed in the bone char at time t, q_e (mg g^{-1}) is its value at equilibrium and k_2 (g mg^{-1} min^{-1}) is a constant of the pseudo-second-order adsorption model. The equilibrium adsorption capacity q_e and the second-order constants k_2 were determined experimentally from the slope and the intercept of plot t/q_t *versus* t, respectively. In general, the pseudo-second order model is used to describe chemisorption mechanisms (Ho, 2006).

The effect of solid/liquid ratio on the adsorption kinetics of manganese is shown in Figure 4.4a and 4.4b for the laboratory solution containing only manganese and for the AMD effluent, respectively. As expected, a higher percentage of manganese removal was obtained with the increase on the solid/liquid ratio for both solutions. Also, the time required to load the adsorbent increased with the increase on the solid/liquid ratio. The effect of competing species present in the AMD effluent for the adsorbent is shown in Figure 4.4b, resulting in a significant reduction on the manganese removal when compared with laboratory solution containing only manganese. Such result points out the necessity to raise the pH of the effluent before treatment in order to increase the loading of the bone char for the specific removal of manganese. The effect of competing species was verified also in the calculated q_e shown in Table IV.3. In fact, smaller values were obtained when the AMD effluent was used, as well as with the increase on the solid/liquid ratio for both solutions as expected. The final pH values of the solutions were kept constant in the range of 7.2 to 7.4 due to the buffer effect from the calcite dissolution.

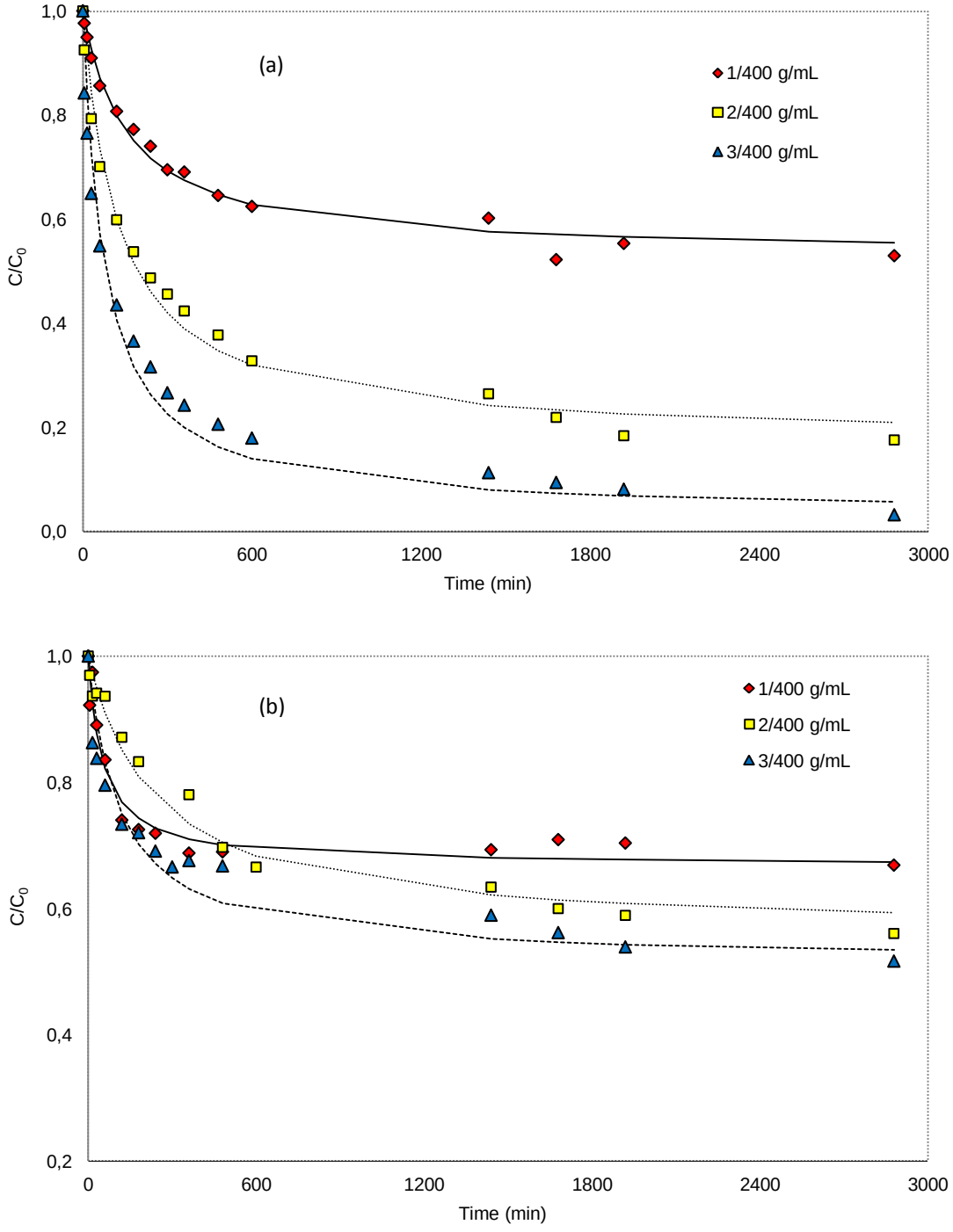

Figure 4.4: Effect of solid/liquid ratio on the kinetics of manganese removal with bone char from (a) laboratory solution (C_0 = 100 mg L^{-1}, pH_i = 5.76), and (b) AMD effluent (25°C, 150 min^{-1}, pH_i = 2.96, 417-833 µm, continuous curves are pseudo-second order model).

Table IV.3: Parameters of pseudo-second order model for the effect of solid/liquid ratio (25°C, 150 min^{-1}, 417-833 µm, pH_i = 5.5-5.7, C_0 = 100 mg L^{-1} in the laboratory solution).

	Solid/liquid ratio (g mL^{-1})	q_e (mg g^{-1})	k_2 x 10^3 (mg g^{-1} min^{-1})	R^2
Laboratory solution	1/400	19	0.33	0.99
	2/400	17	0.48	0.99
	3/400	13	1.00	0.99
AMD effluent	1/400	14	1.30	0.99
	2/400	10	0.44	0.98
	3/400	7	1.20	0.99

Regarding the effect of particle size, the results obtained for laboratory solution (Figure 4.5a) and AMD effluent (Figure 4.5b) revealed that the different particle size ranges studied have little effect in the manganese adsorption at longer times but loading kinetics is affected as expected. As expected, the higher k_2 values for smaller particle size indicated that the time to reach the equilibrium is shorter for the smaller particle size. Once again the effect of competing species present in the AMD effluent for the adsorbent is shown in Figure 4.5b, resulting in a significant reduction on the manganese removal. The values of q_e obtained for different particle sizes are close, as indicated in Table IV.4. The final pH of the solution was kept constant in the range of 7.2 to 7.5.

Ozawa *et al*. (2003) used fish bone hydroxyapatite for manganese removal from laboratory solution. The initial concentration of Mn(II) was 16 mg L^{-1} and 0.3 g of the bone powders was added to each 2 L of aqueous solution. After the mixture of powder and solution to be stirred for 2 hours and held for 6 days without stirring, the maximum adsorption capacity reached was 17 mg g^{-1}. This value of maximum loading is close to the values obtained in this kinetic study for manganese removal using bone char.

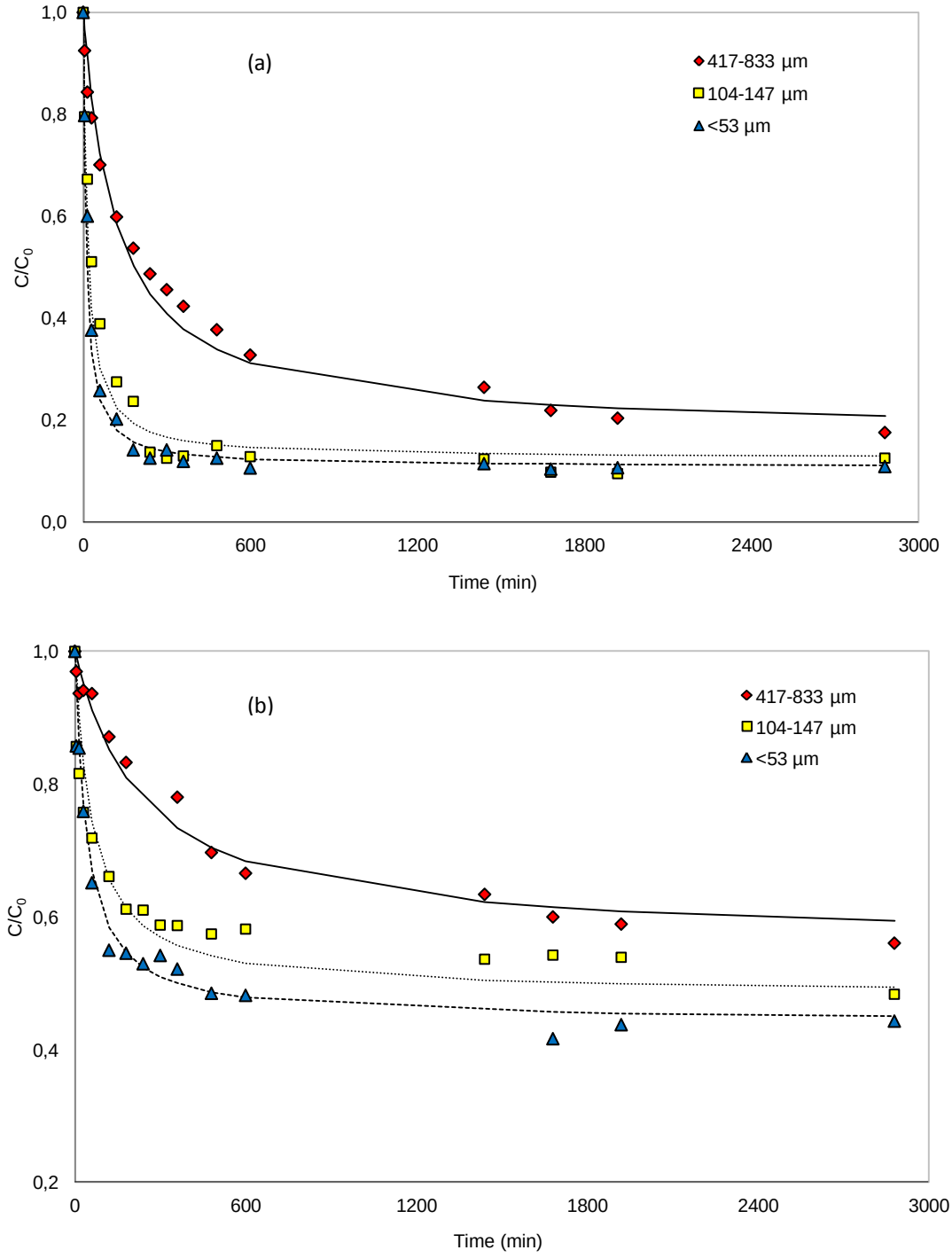

Figure 4.5: Effect of particle size on the kinetics of manganese removal with bone char from (a) laboratory solution (C_0 = 100 mg L^{-1}, pH_i = 5.76), and (b) AMD effluent (25°C, 150 min^{-1}, pH_i = 2.96, 2/400 g mL^{-1}, continuous curves are pseudo-second order model).

Table IV.4: Parameters of pseudo-second order model for the effect of particle size (25℃, 150 min^{-1}, 2/400 g mL^{-1}, pH_i = 5.5-5.7, C_0 = 100 mg L^{-1} in the laboratory solution).

	Particle size (µm)	q_e (mg g^{-1})	$k_2 \times 10^3$ (mg g^{-1} min^{-1})	R^2
Laboratory solution	417-833	17	0.51	0.99
	104-147	18	3.80	0.99
	<53	18	5.60	0.99
AMD effluent	417-833	10	0.44	0.98
	104-147	10	1.60	0.99
	<53	13	2.00	0.99

4.3.3. Batch sorption isotherms

The Langmuir adsorption isotherm which is based on a theoretical model (Gibbs equation) was adequate to fit experimental data of manganese adsorption onto bone char for the conditions investigated. The saturation monolayer can be represented by the following linearized expression:

$$\frac{1}{q_e} = \frac{1}{q_m} + \frac{1}{bq_mC_e} \tag{4.2}$$

in which q_e (mg g^{-1}) is the adsorption capacity by weight at equilibrium, $\underline{q_m}$ (mg g^{-1}) is the theoretical maximum adsorption capacity by weight, b (L mg^{-1}) represents the Langmuir constant, and C_e (mg L^{-1}) is the concentration of adsorbate in the aqueous phase at equilibrium (Annadurai *et al.*, 2008).

The effect of initial pH of the AMD effluent on the removal of manganese is shown in Figure 4.6. As indicated by the equilibrium data, it is observed that the removal of manganese is more effective when the initial pH of the effluent was raised to 6.5 due to precipitation of some metals present in the liquor. Preliminary tests has pointed out that pH range 7.0-7.5 would be ideal for the adsorption of manganese. However, when the

initial pH of effluent was set to 5.0 the final pH was 6.0, and when the initial pH was 6.5 its final value was 7.4, thus attending CONAMA 357 (see Table IV.2) in both situations. The raise on pH during contact of AMD effluent with bone char is attributed to the dissolution of calcite ($CaCO_3$) present in the adsorbent. Therefore, for the solid/liquid ratio used in this experiment, initial pH = 6.5 has a higher value of q_m for the manganese adsorption, as shown in Table IV.5. For laboratory solution, the effect of the initial pH was not studied because it was not necessary to adjust it.

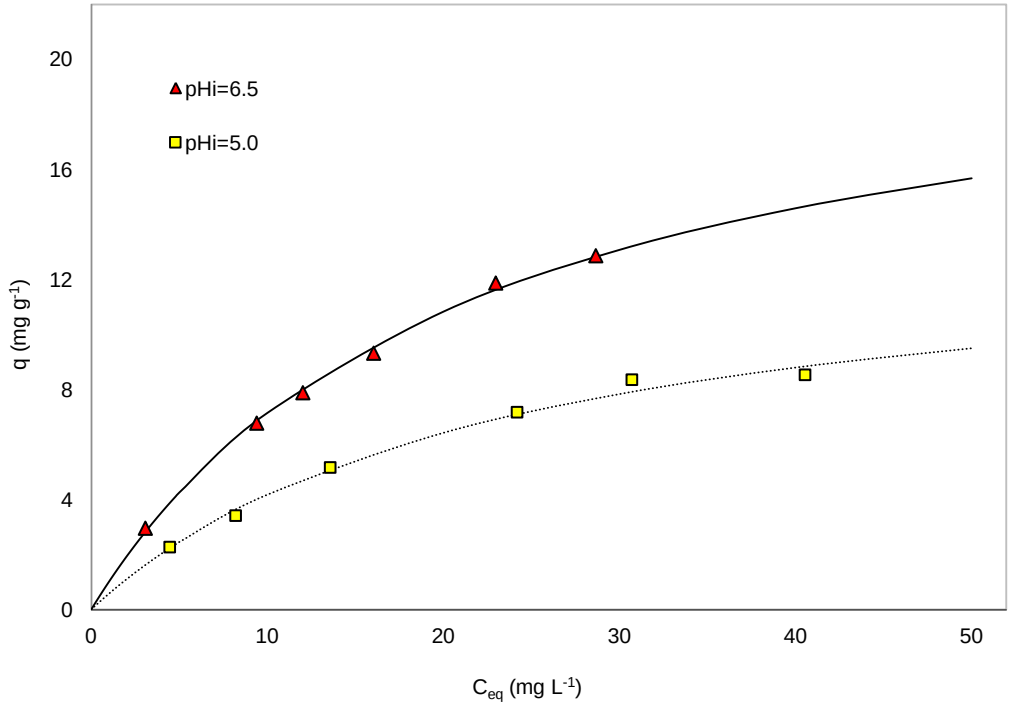

Figure 4.6: Effect of initial pH on the isotherm of manganese removal from AMD effluent with bone char (25°C, 150 min^{-1}, 53 µm, 0.25/100 g mL^{-1}, 48 hours; continuous lines are Langmuir model).

Table IV.5: Parameters of Langmuir equation for the pH effect for AMD effluent (25°C, 150 min^{-1}, <53 µm, 0.25/100 g mL^{-1}, 48 hours).

pH_i	pH_f	q_m (mg g^{-1})	b x 10 (L mol^{-1})	R^2
5.0	6.0	14	0.43	0.98
6.5	7.4	22	0.47	0.99

The effect of temperature on the manganese removal from laboratory solution and from AMD effluent shown in Figure 4.7 revealed that such parameter has little effect in the manganese adsorption for the range investigated as shown in Table IV.6. Therefore, it is expected that manganese removal with bone char is not significantly affected by the seasonal temperature changes in the region where AMD is generated.

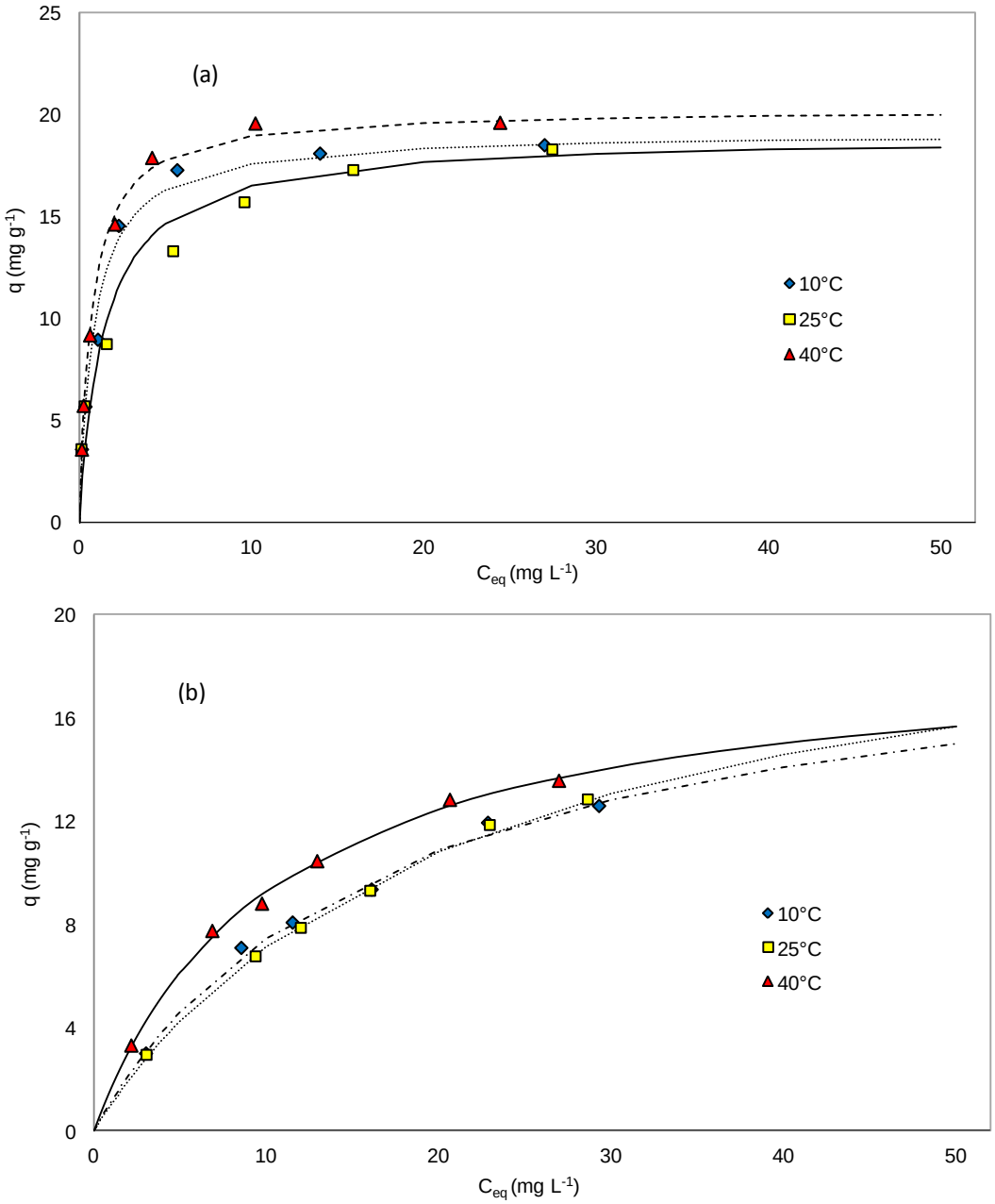

Figure 4.7: Effect of temperature on the isotherm of manganese removal with bone char from (a) laboratory solution (C_0 = 100 mg L^{-1}), and (b) AMD effluent (150 min^{-1}, < 53 µm, 1/400 g mL^{-1}, 48 hours; continuous lines are Langmuir model).

Table IV.6: Parameters of Langmuir equation for the effect of temperature (150 min^{-1}, pH_i = 5.5-5.7, < 53 µm, 1/400 g mL^{-1}, 48 hours).

	Temperature (°C)	q_m (mg g^{-1})	b x 10 (L mol^{-1})	R^2
Laboratory solution	10	19	12.0	0.99
	25	19	6.8	0.99
	40	20	14.0	0.99
AMD effluent	10	20	0.59	0.99
	25	22	0.47	0.99
	40	19	0.96	0.99

Gonçalves (2006) reported the use of bone char in alkaline medium for manganese removal. 22% of manganese present in AMD effluent was removed using 0.2 g of bone char and 200 mL of effluent for an initial concentration of 173 mg L^{-1}. The maximum loading was 38 mg g^{-1} and was bigger than the maximum loading shown in Table IV.6.

The liquor obtained from the effect of temperature study at 25°C was also used to evaluate the adsorption of fluoride species onto bone char. The results shown that after contact with bone char, in the conditions describe above, the fluoride concentration in the AMD effluent are in agreement with the Brazilian legislation and it was smaller than the detection limit of the technique used for this analyze (<0.6 mg L^{-1}).

4.3.4. Mechanism for the removal of manganese with bone char

Cations removal from aqueous solutions by hydroxyapatite may generally occur due to different sorption processes (adsorption, ion-exchange, surface complexation, co-precipitation, recrystalization) depending on the experimental conditions and on the nature of both sorbing cations and hydroxyapatite itself. Smiciklas *et al*. (2000) reported that acidic as well as basic solutions in pH range 4–10 can be buffered after reaction with the reactive surface sites of hydroxyapatite to its pH_{pzc} value in which the surface charge is zero.

According to Pan *et al*. (2009), the surface charge of the hydroxyapatite is predominated by positively charged ≡ $CaOH_2^+$ and neutral ≡ POH^0 species in acidic solutions, so the surface charge of hydroxyapatite in this pH conditions is positive. On the other hand, in alkaline solutions, neutral ≡ $CaOH^0$ and negatively charged ≡ PO^- species may prevail on the hydroxyapatite surface, so it becomes negatively charged:

$$\equiv CaOH_2^+ \leftrightarrows \equiv CaOH^0 + H^+ \quad (4.3)$$

$$\equiv PO^- + H^+ \leftrightarrows \equiv POH^0 \quad (4.4)$$

The electrical characteristics of bone char was evaluated from measurements of zeta potential by Rocha *et al*. (2011) and the results pointed out that the surface of bone char is predominated by negatively charged in pH values above 5. This fact can increase the electrostatic attraction forces between the bone char surface and the cations from the solution, thus favoring the sorption of cations from aqueous solutions with pH > 5.

For investigate the release of calcium in solution, the bone char was washed as described by Ribeiro (2011) in order to dissolve the calcite present in the material. The calcium in solution (Figure 4.8) showed that ion exchange was involved in the removal of manganese from AMD for this initial manganese concentration range. According to O'Connor and Weatherley (1997), the hydroxyapatite component of the bone char plays an important role in the adsorption of manganese, with adsorption occurring by ion exchange. There was good linear relationship (R^2 = 0.95) between the release of calcium into solution and the manganese adsorbed to bone char.

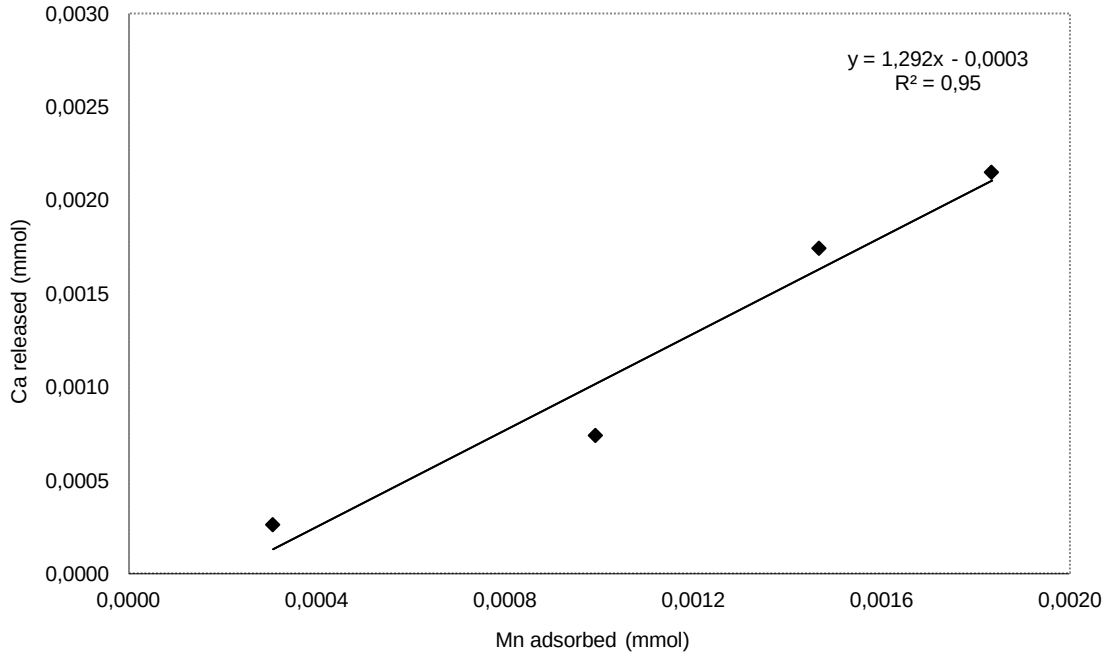

Figure 4.8: Relationship between release of calcium into solution and manganese adsorbed to bone char (25°C, 150 min^{-1}, 417–833 µm, 0.25/100 g mL^{-1}, pH_i = 5.76, C_0 = 100 mg L^{-1}, 24 hours).

The effect of diffusion as the rate controlling mechanism in the manganese removal by bone char was evaluated according to the intraparticle diffusion model. It is known that intraparticle diffusion plays a significant role in many adsorption processes and normally the most significant contribution for the kinetic-mass transfer process is due to the diffusion of adsorbate within the pore structure of the adsorbent. The intraparticle diffusion model for adsorption is given by the following equation (Weber and Morris, 1963):

$$q_t = k_p \sqrt{t} + C \tag{4.5}$$

in which k_p is the intraparticle diffusion constant which is evaluated as the slope of the curve q_t *versus* $t^{1/2}$ and C is the constant related to the boundary layer thickness. If the regression of q_t *vs.* $t^{1/2}$ is linear and passes through the origin, then intraparticle diffusion is the sole rate-limiting step.

In order to evaluate the effect of intraparticle diffusion in the manganese adsorption process, the q_t was plotted as a function of square root of time, $t^{1/2}$ at different granulometry for laboratory solution and AMD effluent (see Figure 4.9). The plot for intraparticle diffusion revealed a linear behavior passing near to the origin at the beginning of manganese adsorption process (until 180 min for the particle size range of <53 and 104-147 µm, and until 600 min for the particle size range of 417-833 µm). It indicates that intraparticle diffusion is the main rate-limiting step for manganese sorption systems but not the sole rate-limiting step since the plot for intraparticle diffusion pass near to the origin. The k_p values shown in Table IV.7 reveal that intraparticle diffusion becomes slower when the particle size increases. This may occur due to the fact that the particle size range of 417-833 µm has a major contribution of smaller pores (Table IV.1) than the others particle size ranges studied in this work. It may difficult the intraparticle diffusion of the metal, so manganese removal becomes slower. The C constant values indicate that, the larger the intercept the greater the boundary layer effect (Annadurai *et al*., 2008). Based on the results shown in Table IV.7, the effect of external resistance increased when smaller particle size were used.

Table IV.7: Parameters of intraparticle diffusion model for manganese adsorption on bone char (25°C, 150 min^{-1}, 2/400 g mL^{-1}, pH_i = 5.5-5.7, C_0 = 100 mg L^{-1} in the laboratory solution).

	Particle size (µm)	k_p (mg g^{-1} $min^{-0.5}$)	C (mg g^{-1})	R^2
Laboratory solution	417-833	0.53	1.41	0.97
	104-147	1.00	3.10	0.93
	< 53	1.06	2.02	0.99
AMD effluent	417-833	0.29	0.05	0.98
	104-147	0.44	2.21	0.98
	< 53	0.66	1.95	0.95

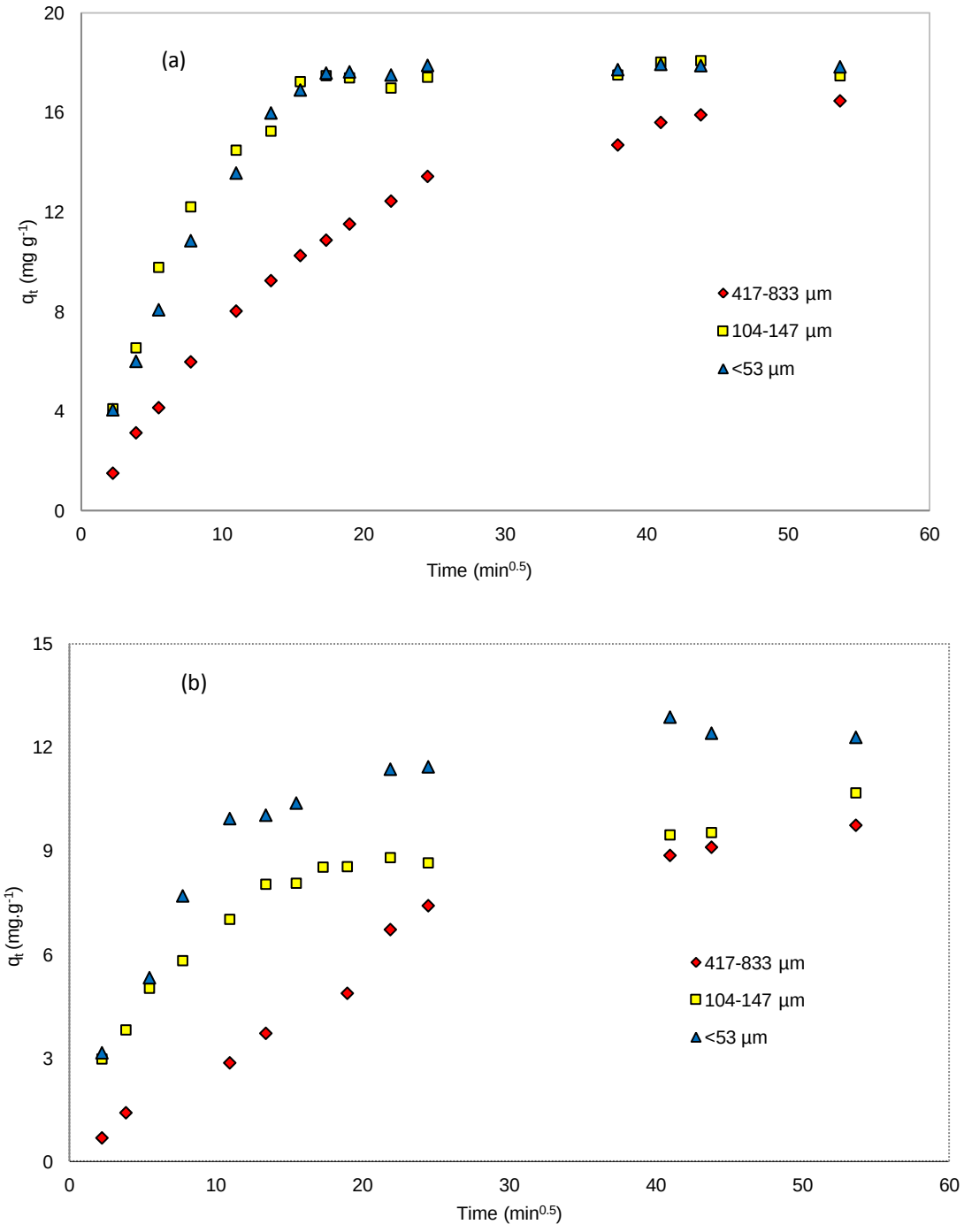

Figure 4.9: Intraparticle mass transfer for manganese removal with bone char from (a) laboratory solution (C_0 = 100 mg L^{-1}), and (b) AMD effluent (25°C, 150 min^{-1}, 2/400 g mL^{-1}).

4.4. Conclusions

In this study, batch equilibrium and kinetics tests were carried out to evaluate the feasibility of using bone char for the removal of manganese from AMD effluents. Experiments using a laboratory solution containing manganese at typical concentrations were also done for comparative analysis. The following main conclusions can be drawn based on the results obtained:

- Equilibrium data was adequately described by the Langmuir model and the maximum value of q_m for manganese adsorption was 22 mg g^{-1} for AMD effluent and 20 mg g^{-1} for laboratory solution;
- Kinetic tests revealed that manganese removal by bone char is relatively slow (equilibrium is reached after at least 600 minutes). It was verified also that manganese loading follows a pseudo-second order model, thus indicating the existence of a chemisorption mechanism probably involving an ion exchange process between manganese and calcium ions;
- The effect of competing species present in the AMD effluent for the bone char is significant, so the pH of effluent must be previously raised to near neutral condition to precipitate the other metals before contact with bone char. For instance, at initial pH = 6.5, manganese removal of up to 70% was achieved, while at initial pH = 5.0 the removal was lower than 50%.
- The final concentration of fluoride and others metals present in the AMD effluent was in agreement with the limit concentration established by Brazilian legislation (CONAMA, 2005);
- A relatively small effect of operating variables temperature and particle size was verified for the investigated operating conditions, and;
- The diffusion inside particles was identified as the main rate-limiting step for manganese removal. However, when particles of smaller sizes are used, external mass transfer and intraparticle diffusion contributions may affect manganese removal.

Comparing with the current treatment of AMD effluents by precipitation with lime, a smaller volume of sludge is expected. According to Carvalho *et al*. (2009), the removal of manganese at pH close to the neutrality reduces by 50% the volume of

precipitate generated in the treatment of the effluent. In addition, the buffer effect of the bone char may avoid the need for pH correction of effluent after treatment. Therefore, the removal of manganese from AMD effluents using bone char as adsorbent was found to be technically feasible and more efficient removal rates of manganese are expected with the use of bone char in continuous column operations.

4.5. Acknowledgements

The authors acknowledge the financial support from FAPEMIG, CNPq, CAPES and INCT-Acqua: National Institute of Science and Technology of Mineral Resources, Water and Biodiversity. The authors also acknowledge the contribution from Bone Char do Brasil Ltda as well as Prof. Sônia Denise Ferreira Rocha (DEMIN/UFMG) and Prof. Ana Cláudia Ladeira (CDTN) for the fruitful discussion and contribution.

4.6. References

ANNADURAI, G.; LING, L.Y.; LEE, J.F. Adsorption of reactive dye from solution by chitosan: isotherm, kinetic and thermodynamic analysis. *Journal of Hazardous Materials*, v. 152, p. 337-346, 2008.

BAMFORTH, S.M.; MANNING, D.A.C.; SINGLETON, I.; YOUNGER, P.L.; JOHNSON, K.L. Manganese removal from mine waters – investigating the occurrence and importance of manganese carbonates. *Applied Geochemistry*, v. 21, p. 1274-1287, 2006.

BOSCO, S.M.D.; JIMENEZ, R.S.; CARVALHO, W.A. Removal of toxic metals from wastewater by Brazilian natural scolecite. *Journal of Colloid and Interface Science*, v. 281, p. 424-431, 2005.

CARVALHO, G.X.; AGUIAR, A.O.; LADEIRA, A.C.Q. Estudo da remoção de manganês de efluentes líquidos por precipitação. In: Proc. of the XXIII Encontro Nacional de Tratamento de Minérios e Metalurgia Extrativa, Gramado, Brazil (in Portuguese), 2009.

CHEN, Y.-N.; CHAI, L.-Y.; SHU, Y.-D. Study of arsenic(V) adsorption on bone char from aqueous solution. *Journal of Hazardous Materials*, v. 160, p. 168-172, 2008.

CHEUNG, C.W.; PORTER, J.F.; McKAY, G. Sorption kinetics for the removal of copper and zinc from effluents using bone char. *Separation and Purification Technology*, v. 19, p. 55-64, 2000.

CHOY, K.K.H.; KO, D.C.K.; CHEUNG, C.W.; PORTER, J.F.; MCKAY, G. Film and intraparticle mass transfer during the adsorption of metal ions onto bone char. Journal *of Colloid and Interface Science*, v. 271, p. 284-295, 2004.

CONSELHO NACIONAL DO MEIO AMBIENTE. Resolução CONAMA n.º 357/2005: Classificação dos corpos de água e diretrizes ambientais para o seu enquadramento, bem como estabelece as condições e padrões de lançamento de efluentes. Brasília, 2005. Disponível na Web em: http://www.mma.gov.br/port/conama/index.cfm.

GONÇALVES, C.R. Remoção de manganês e recuperação de urânio presentes em águas ácidas de mina. Belo Horizonte, 2006. Dissertação (Mestrado) - Centro de Desenvolvimento da Tecnologia Nuclear.

HASSAN, S.S.M; AWWAD, N.S.; ABOTERIKA, A.H.A. Removal of mercury(II) from wastewater using camel bone charcoal. *Journal of Hazardous Materials*, v. 154, p. 992-997, 2008.

HO, Y.S. Review of second-order models for adsorption systems. *Journal of Hazardous Materials*, B136, p. 681-689, 2006.

KORN, M.G.A., SANTOS JR., A.F., JAEGER, H.V., SILVA, N.M.S., COSTA, A.C.S., 2004. Cooper, zinc and manganese determination in saline samples employing FAAS after separation and preconcentration on Amberlite XAD-7 and Dowex 1X-8 loaded with alizarin Red. *Journal of Brazilian Chemical Society*, v. 15(2), p. 212-218.

NASCIMENTO, M.R.L. Remoção e recuperaçâo de urânio de águas ácidas de mina por resina de troca iônica. São Carlos, 1998. Dissertação (Mestrado) - Universidade Federal de São Carlos.

PAN, X.; WANG, J.; ZHANG, D. Sorption of cobalt to bone char: kinetics, competitive sorption and mechanism. *Desalination*, v. 249, p. 609-614, 2009.

ROBINSON-LORA, M.A.; BRENNAN, R.A. Biosorption of manganese onto chitin and associated proteins during the treatment of mine impacted water. *Chemical Engineering Journal*, v. 162, p. 565-572, 2010.

ROCHA, S.D.F.; RIBEIRO, M.V.; VIANA, P.R.M.; MANSUR, M.B. Bone char: an alternative for removal of diverse organic and inorganic compounds from industrial wastewater. In: Bhatnagar, A. (Org.), Application of adsorbents for water pollution, Bentham Science Publishers Ltd., Ch. 14 (in press), 2011.

SMICIKLAS, I.D.; MILONJIC, S.K.; PFENDT, P.; RAICEVIC, S. The point of zero charge and sorption of cadmium (II) and strontium (II) ions on synthetic hydroxyapatite. *Separation and Purification Technology*, v. 18, p. 185-194, 2000.

SOTO, O.A.J.; TOREM, M.L.; TRINDADE, R.B.E. Palygorskite as a sorbent in the removal of manganese(II) from water mine effluents. In: XIII INTERNATIONAL CONFERENCE ON HEAVY METALS IN THE ENVIRONMENT, Rio de Janeiro - RJ, 2005.

WEBER, W.J.; MORRIS, J.C. Kinetic of adsorption carbon solution, *Journal Sanitary Engineering Divisor*, American Society Civil Engineers v. 89, p. 31-59, 1963 *apud* ANNADURAI, G.; LING, L.Y.; LEE, J.F. Adsorption of reactive dye from solution by chitosan: isotherm, kinetic and thermodynamic analysis. *Journal of Hazardous Materials*, v. 152, p. 337-346, 2008.

5. ADSORPTION OF MANGANESE FROM ACID MINE DRAINAGE EFFLUENTS USING BONE CHAR: CONTINUOUS FIXED BED COLUMN AND BATCH DESORPTION STUDIES.

Dalila Chaves Sicupira [a], Thiago Tolentino Silva [a], Ana Cláudia Queiroz Ladeira [b] and Marcelo Borges Mansur [a,*].

[a] Departamento de Engenharia Metalúrgica e de Materiais, Universidade Federal de Minas Gerais

Av. Antônio Carlos, 6627, Campus Pampulha, 31270-901, Belo Horizonte, MG, Brazil

Tel.: +55 (31) 3409-1811; Fax: +55 (31) 3409-1716

E-mail: marcelo.mansur@demet.ufmg.br

* Corresponding author.

[b] Centro de Desenvolvimento da Tecnologia Nuclear, CNEN.

Av. Antônio Carlos, 6627, Campus Pampulha, 31270-901, Belo Horizonte, MG, Brazil

Abstract

In this study, continuous fixed bed column runs were done aiming to evaluate the feasibility of using bone char for the removal of manganese from acid mine drainage (AMD). Tests using laboratory solution containing solely manganese at typical concentration level were also carried out for comparison purposes. The following operating variables were evaluated: column height, flow rate and initial pH. Significant variations in resistance to the mass transfer of manganese into the bone char were identified using the Thomas model. A significant effect of bed height was observed only in tests with laboratory solution. No significant change on the breakthrough volume was observed with different flow rate. Increasing the initial pH from 2.96 to 5.50, the breakthrough volume was increased. The maximum manganese loading capacity in continuous tests using bone char for AMD effluent was 6.03 mg g^{-1} and for laboratory solution was 26.74 mg g^{-1}. The study included also desorption tests using solutions of HCl, H_2SO_4 and water aiming to reuse the adsorbent but no promising results were obtained due to low desorption levels associated with relatively high mass loss. Despite desorption results, the removal of manganese from AMD effluents using

bone char as adsorbent is technically feasible thus attending environmental legislation. It is interesting to note that the use of bone char for manganese removal may avoid the need for pH correction of effluent after treatment. Also, it can remove fluoride ions and other metals, so bone char is a quite interesting alternative material for the treatment of AMD effluents**.**

Key-words: manganese; bone char; acid mine drainage; continuous fixed bed column; adsorption/desorption.

5.1. Introduction

Among the main environmental aspects and impacts of mining activities, the one associated with the contamination of surface and groundwaters by acid mine drainage (AMD) is probably the most significant one (Nascimento, 1998). AMD generation is normally associated with the presence of sulfides like pyrite (FeS_2), for instance, as verified in the extraction of gold, coal, copper, zinc and uranium. Mining wastes when exposed to oxidizing conditions in the presence of water may generate AMD, therefore the proper disposal of mining wastes from such operations is crucial to prevent and/or minimize its generation (Ladeira and Gonçalves, 2007). Besides waste rock piles, AMD may also occur in open or underground pit mine, tailings storage and ore stockpiles. It often contains high concentrations of SO_4^{2-} ions and the high acidity of such solutions may promote the dissolution of metals like Zn, Cu, Cd, As, Fe, U, Al and Mn (Bamforth *et al*., 2006; Robinson-Lora and Brennan, 2009). Such metal dissolution is probably the most deleterious effect of AMD contamination because the resulting acidic and metal contaminated streams can adversely impact humans and wildlife.

In Brazil, AMD has been highlighted in the mining region of Poços de Caldas, in the state of Minas Gerais. The drainage generated in this region contains radionuclides (U, Th and others) and species like Mn, Zn, Fe and F^- ions at concentration levels above those allowed by Brazilian legislation for direct discharge into the environment (Ladeira and Gonçalves, 2007). The current treatment of such acid waters consists of metals precipitation with lime followed by pH correction. Most of metal species are removed but manganese ions removal from AMD is notoriously difficult to occur due to their

complex chemistry (Bamforth *et al.*, 2006; Robinson-Lora and Brennan, 2010). For complete precipitation of manganese, the pH must be raised to around 11, and such operation involves a significant consumption of lime (Gonçalves, 2006). In addition, after manganese removal, the pH must be neutralized for discharge so such treatment is costly, generates large volumes of sludges and requires the consumption of high quantities of reagents to be effective. New technologies to treat such effluents containing manganese are then urged.

In this context, a promising method based on the removal of manganese using bone char as adsorbent has been recently proposed (Sicupira *et al.*, 2012). According to this method, manganese was quantitatively removed from AMD at pH values near 6-7. As an advantage, no pH correction of the treated effluent is necessary due to the buffer effect of the bone char. Equilibrium and kinetics batch tests revealed that adsorption of manganese with bone char was also influenced by the solid/liquid ratio. The particle size and temperature studied had quite little effect on the manganese adsorption for the operating range evaluated. The maximum value of q_m found for manganese adsorption based on Langmuir model was 22 mg g^{-1}.

In the view of the aforementioned, the aim of this work is to evaluate the feasibility of treating AMD solutions containing manganese with bone char in continuous fixed bed systems, in order to reach the levels required by the Brazilian legislation for direct discharge of effluents. According to CONAMA (2005), the limit of total dissolved manganese concentration in effluents is 1.0 mg L^{-1} and pH around 6-9. Fixed bed tests were carried out using AMD effluents and laboratory solutions containing manganese at typical concentrations for comparative analysis. Desorption studies were carried out also with bone char previously loaded with manganese from laboratory solution in order to evaluate the possibility to reuse it.

5.2. Experimental

5.2.1. Reagents

Bone char supplied by Bone Char do Brasil Ltda was used in this study. It contains basically hydroxyapatite $Ca_{10}(PO_4)_6(OH)_2$ and calcite $CaCO_3$ (Sicupira *et al*., 2012). SEM-EDS analysis has shown a significant presence of calcium and phosphorus, as expected; manganese and others metals were identified on its surface after contact with AMD, thus suggesting that such metals were removed from the effluent possibly due to some adsorptive and/or precipitating process. The main characteristics of the bone char used in this study are as follows: real density = 2.9 g cm^{-3}, total pore volume = 0.275 cm^3 g^{-1}, surface area = 93 m^2 g^{-1} and particle size = 417-833 μm.

The AMD effluent used in this study was collected nearby one closed uranium mine in Poços de Caldas region. Its metal composition is shown in Table V.1, which includes the limit concentration for discharge in Brazil according to CONAMA (2005). It can be seen that manganese concentration in the AMD exceeds the maximum value of Brazilian legislation; the same occurs with zinc and acidity, but not to iron. After precipitation with $Ca(OH)_2$ 30%, manganese concentration was still not in agreement with legislation (see also in Table V.1), so additional treatment is required. Continuous fixed bed column runs using a laboratory solution containing 100 mg L^{-1} of manganese were also carried out for comparative analysis. Such solution was prepared using chemicals of analytical reagent grade dissolved in distilled water.

Table V.1: Chemical characterization of the AMD effluent (Sicupira *et al.*, 2012).

Parameters	Concentration ($mg\ L^{-1}$)	Concentration after precipitation ($mg\ L^{-1}$)	CONAMA 357 ($mg\ L^{-1}$)
U	6.8	<0.3	-
Mn	107.5	89.5	1.0
Ca	104.9	428	-
Mg	7.6	7.4	-
Al	164.2	28.5	-
Zn	17.7	4.0	5.0
Fe	<0.01	<0.01	15.0
F^-	99.0	38.0	10.0
SO_4^{2-}	1349	1335	-
pH*	2.97	5.64	6 to 9

* All parameters are expressed in $mg\ L^{-1}$, except pH.

- Permissible level not defined by the Brazilian legislation.

5.2.2. Instrumentation

Atomic emission spectrometer with inductively coupled plasma (ICP-AES, Perkin Elmer OPTIMA 7300DV) was used for assessing the concentration of manganese in the aqueous solutions. Sulfate, phosphate and fluoride analysis were performed using a DX500 Dionex ion chromatograph. The pH measurements were carried out using a pH meter (Quimis). A scanning electron microscopy (SEM, SEI INSPECT S50) was employed to analyze the surface morphology of the bone char.

5.2.3. Continuous fixed bed column runs

Continuous fixed bed column runs were conducted to determine the adsorption capacity of bone char under continuous flow conditions. All column runs were performed in down flow mode. The column was filled with 40 g of bone char with particle size of 417-833 μm. The effluent (pH_i = 2.96 or 5.50) was continuously fed into the column using a peristaltic pump (Cole-Parmer, Masterflex); in the case of laboratory solution

the pH_i = 5.76 was used. The range of initial pH was chosen based on previous batch equilibrium and kinetics studies (Sicupira *et al*., 2012); the AMD effluent sample has a typical pH value of approximately 3. The diameter of the adsorptive bed of the column was 2.2 cm and a hydraulic flow rate of 7.5 mL min^{-1} was maintained constant. Effluent samples were collected at determined contact times from the column, filtered and acidified using HNO_3 before being analyzed by ICP-AES. The fixed bed studies were also carried out with flow rate of 3.0 mL min^{-1} to evaluate the effect of the flow rate in the fixed bed column and the effect of the mass of bone char was also evaluated using 20 g of bone char. As the temperature did not show significant effect on the adsorption of manganese onto bone char in batch studies (Sicupira *et al*., 2012), all continuous runs were carried out at room temperature. Breakthrough curves were plotted showing the concentration ratio C_t/C_0 (manganese concentration at time t divided by the initial concentration of manganese) versus the number of bed volumes (BV), which is defined as the eluted volume divided by the volume of bed's voids (Cussler, 1997).

5.2.4. Modeling

The Thomas model was chosen to evaluate the adsorption characteristics of manganese from AMD effluents in continuous column operation due to its simplicity. It is widely used in the modeling of fixed bed breakthrough curves (Unuabonah *et al*., 2010). The model assumes a Langmuir (favorable) isotherm in accordance to previous investigation on the adsorption of manganese onto bone char (Sicupira *et al*., 2012) and it is given by the following equation (Chu, 2010):

$$\frac{C_t}{C_0} = \frac{1}{1+\exp\left(k_T\left(\frac{q_0 M}{Q} - C_0 t\right)\right)} \tag{5.1}$$

The linearized form of Thomas model can be expressed as follows:

$$n\left(\frac{C_0}{C_t} - 1\right) = \frac{k_T q_0 M}{Q} - k_T C_0 t \tag{5.2}$$

in which k_T (L mg^{-1} min^{-1}) is the Thomas rate constant, q_0 is the sorption capacity of the adsorbent per unit mass (mg g^{-1}), M is the mass of adsorbent (g) and Q is the flow rate

(L min^{-1}). The kinetic coefficient k_T and the adsorption capacity q_0 can be obtained from the plot of $\ln\left(\frac{C_0}{C_t} - 1\right)$ against time (t) at a given flow rate using linear regression (Cavas *et al*., 2011).

5.2.5. Desorption studies

Metal desorption was evaluated using selected eluents: HCl (0.01M, 0.001M, 0.0001M), H_2SO_4 (0.01M, 0.001M, 0.0001M) and H_2O. Desorption was carried out by contacting a loaded sorbent (500 mg, dry weight, previously saturated with metals, obtained from batch adsorption experiments) with a given volume of eluent (100 mL) under agitation (150 rpm) at 25ºC using a mechanical shaker (INNOVA 44). Samples (1 mL) were collected at fixed contact times, diluted and filtered before being analyzed by ICP-AES.

5.3. Results and Discussion

5.3.1 Fixed bed sorption runs

The effect of bed height on the sorption of manganese in the continuous fixed bed column is shown in Figure 5.1. Analyzing the curves obtained, the breakthrough curves for the laboratory solution did not show the typical "S" shape (see Figure 5.1a) as verified in runs with AMD effluent (see Figure 5.1b). In fact, the curves obtained in the runs with laboratory solutions are more inclined to the right. Such behavior is an indicative that the mass-transfer zone is almost as long as the bed and that significant resistance are involved, so a longer period of time is necessary to reach the saturation point (Quek and Al-Duri, 2007) and less than one-half of the bed capacity is utilized (McCabe *et al.*, 2005). The difference in the shape of the curves is due to the distinct flow rates used in the runs. According to Gonçalves (2006), the breakthrough curve is sharper with the increasing of the adsorption rate, i.e., at lower flow rates and lower initial concentration of feed solution.

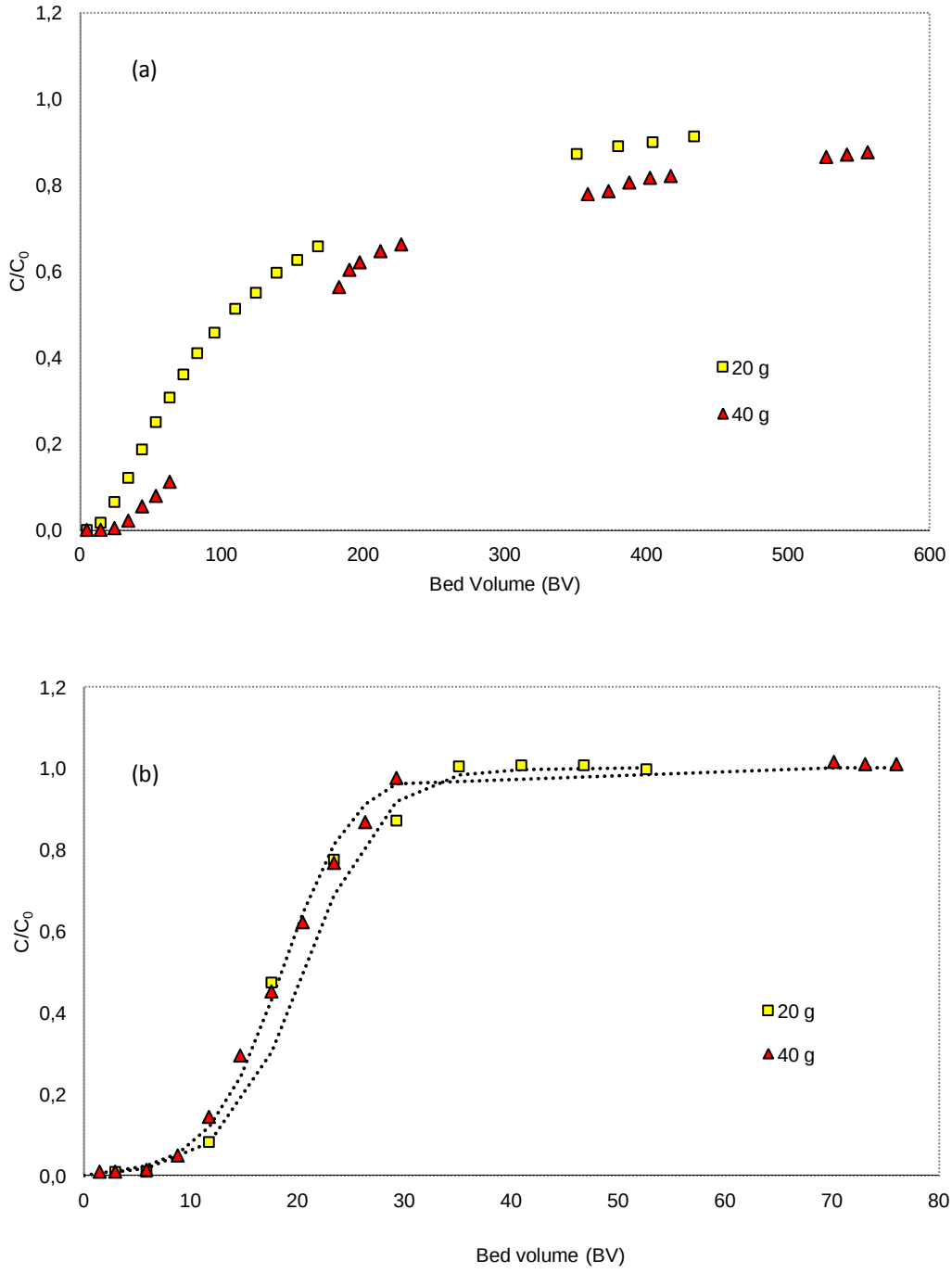

Figure 5.1: Effect of bed height on the breakthrough of manganese removal with bone char in a continuous fixed bed column (417-833 µm): (a) Laboratory solution (flow rate = 7.5 mL min^{-1}, C_0 = 100 mg L^{-1}, pH_i = 5.76), (b) AMD effluent (flow rate = 3.0 mL min^{-1}, pH_i = 2.96, continuous curves are Thomas model).

The constants of Thomas model (k_T and q_0) and operating parameters BV_b (breakthrough point that refers to the maximum manganese concentration in effluents limited by CONAMA at 1.0 mg L^{-1}) and BV_s (saturation point that refers to final manganese concentration is equal to the initial manganese concentration) for laboratory solution and AMD effluent are shown in Table V.2. Results for laboratory solution reveal that an increase in the mass of bone char increases the breakthrough point. Increasing the mass of bone char from 20 g to 40 g, at a constant flow rate, the breakthrough time was extended from 50 min to 280 min and the number BV_b was extended from 11.70 to 34.16 due to the increasing in the number of binding sites. In the case of AMD effluent, increasing the mass of bone char from 20 g to 40 g, at a constant flow rate, the breakthrough time was extended from 60 min to 120 min, but the number BV_b was unchanged; in fact, the same value of 5.85 for both mass of bone char was obtained and it was smaller than the BV_b values obtained for the laboratory solution. This can be attributed to the fact that, in the case of AMD effluent (pH_i = 2.96), the initial pH is lower and that there are others species in solution that may limit the removal of manganese. A precipitate formed on the surface of the loaded bone char can be seen in Figure 5.2 that probably blocked the binding sites, preventing the progressing of the removal process. In the case of AMD effluent, is also interesting to note that the pH of the effluent that leave the column dropped quickly thus reducing manganese adsorption.

Concerning the values of rate constant of Thomas model (k_T) and the maximum loads (q_0) shown in Table V.2, quite different values were obtained for k_T for both solutions, which means there are significant variations in resistance to the mass transfer into the bone char for both systems. The q_0 values are bigger for the longer bed height in the laboratory solution due to the increasing in the number of binding sites. For AMD effluent, the q_0 values are approximately the same, since the manganese removal was limited by the precipitate formed on the bone char surface and the low pH value of the effluent that leave the column and not by the binding sites. As can be seen by comparing Figure 5.1 and Table V.2, the higher the value of the constant k_T, the more effective is the mass transfer process, thus resulting on sharper “S” curves.

Table V.2: Parameters of Thomas model for the adsorption of manganese onto bone char (417-833 µm).

	Mass of bone char (g)	Flow rate (mL min^{-1})	initial pH	final pH	BV_b	BV_s	q_0 (mg g^{-1})	k_T x10^4 (mg g^{-1} min^{-1})	R^2
Laboratory solution	20	3.0	5.76	7.34	11.70	444.60	15.97	0.23	0.95
	20	7.5	5.76	7.34	11.70	444.60	15.85	0.44	0.95
	40	7.5	5.76	7.34	34.16	556.35	26.74	0.24	0.99
AMD effluent	20	3.0	2.96	4.45	5.85	35.09	2.85	3.00	0.97
	20	3.0	5.50	5.55	17.55	70.19	6.03	1.32	0.97
	40	3.0	2.96	4.45	5.85	35.09	2.60	1.58	0.99

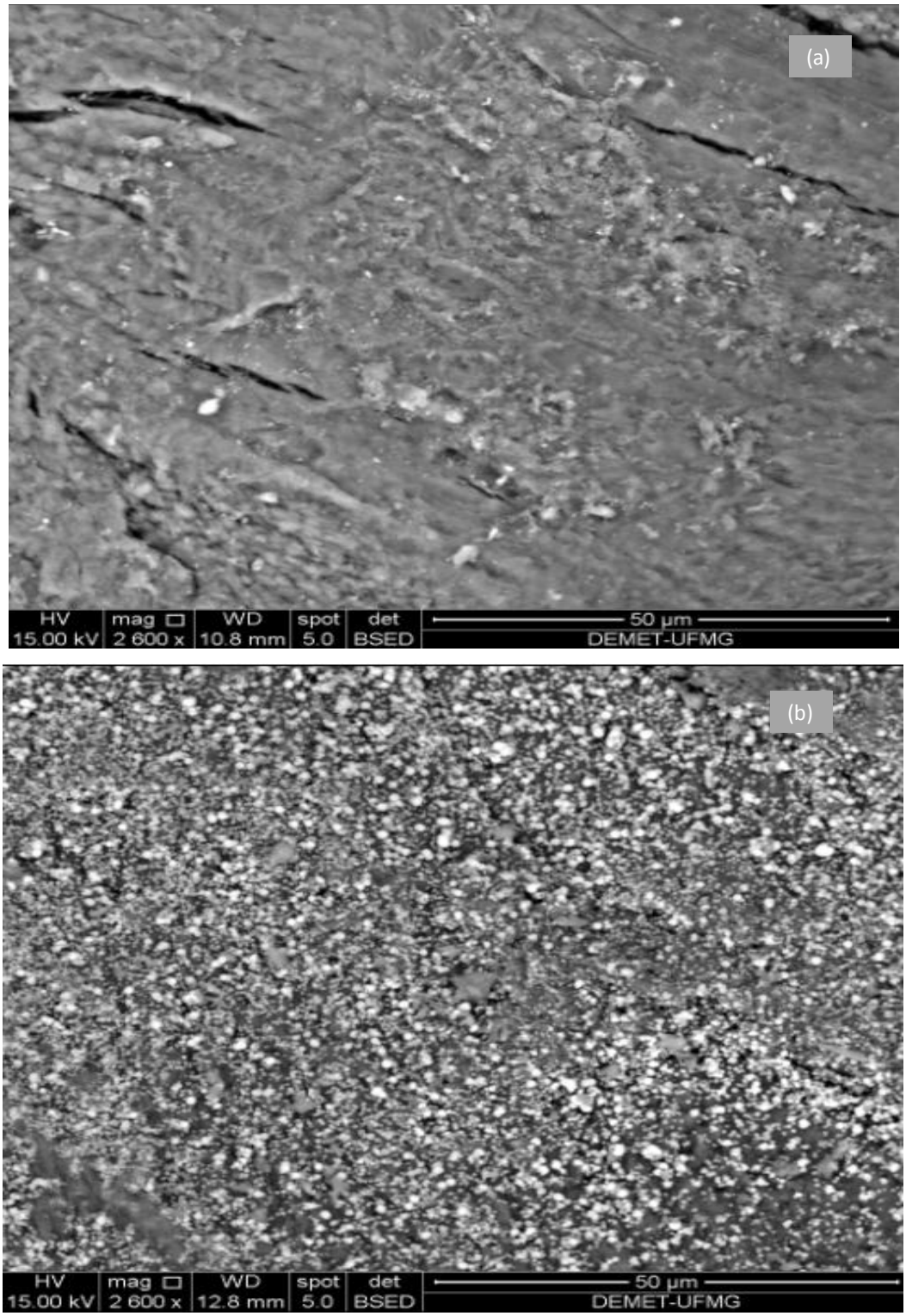

Figure 5.2: Morphology of bone char by SEM (scanning electron microscopy): (a) bone char as received, and (b) bone char after contact with AMD effluent in the column.

The effect of flow rate on the manganese removal in the continuous fixed bed column is shown in Figure 5.3. No significant change on the breakthrough point was verified with the increase in the evaluated flow rate range. As expected, faster saturation of the bed was obtained with the increase of the flow rate from 3.0 mL min^{-1} to 7.5 mL min^{-1}, at a same bed height. The BV_b was also the same value of 11.70 because it is limited by the number of binding sites.

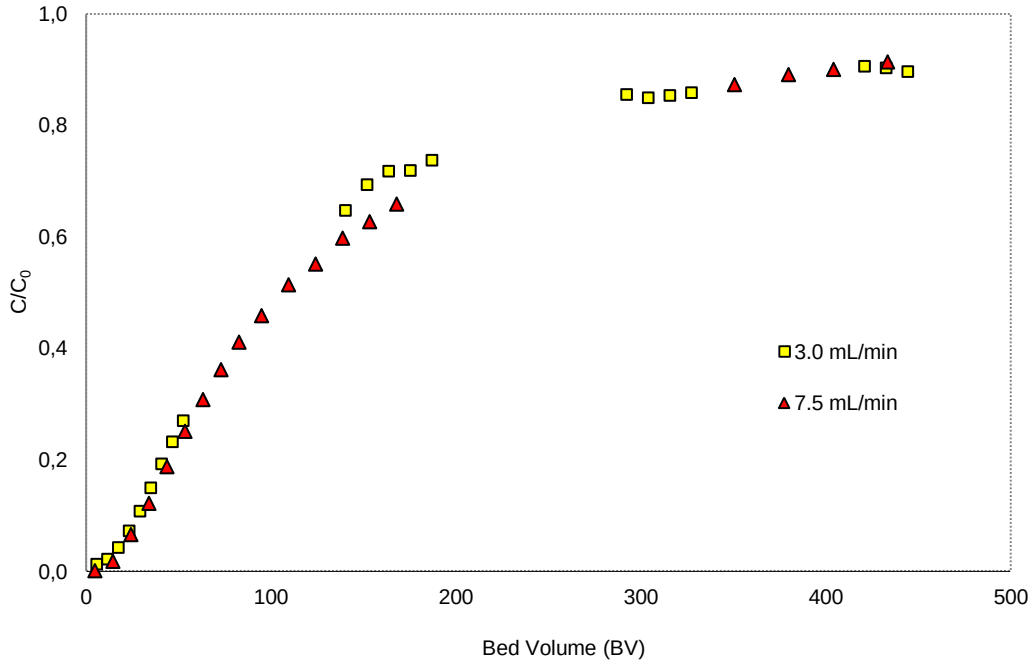

Figure 5.3: Effect of flow rate on the breakthrough of manganese removal with bone char in a continuous fixed bed column using the laboratory solution (C_0 = 100 mg L^{-1}, pH_i = 5.76, mass = 20 g, 417-833 µm).

The effect of the initial pH of AMD effluent was also evaluated and results are shown in Figure 5.4. Increasing the initial pH from 2.96 to 5.50, at the same operating conditions, is possible to observe that the saturation point is quickly reached for the pH_i = 2.96, due to the fact that the pH value of the effluent that leaves the column dropped from approximately 8.0 to 2.96 in a few minutes. The saturation point occurred after 240 min for pH_i = 2.96 and after 660 min for pH_i = 5.50. As observed by Sicupira *et al.* (2012), manganese adsorption does not occur in low pH values. In fact, increasing the initial pH from 2.96 to 5.50, at a constant flow rate, the breakthrough time was extended from 360

min to 720 min, and the number of BV_b was extended from 35.09 to 70.19. Regarding the values of Thomas model shown in Table V.2, the value obtained to q_0 is bigger for pH_i = 5.50 than for pH_i = 2.96, since the manganese adsorption is favored by the progressing of the pH value during the experiment at pH_i = 5.50. Moreover, the AMD effluent at pH_i = 2.96, has other metals ions in solution that compete with manganese for binding sites. This can occur or by the competition of the other metals ions with manganese or by formation of precipitate of these metals ions on the bone char surface that can block the binding sites. As no work was found in the literature using bone char as adsorbent for the removal of manganese in fixed bed columns, no comparison of the results obtained in this study was possible. The maximum manganese loading calculated in continuous tests using bone char was 6.03 mg g^{-1} for AMD effluent and 26.74 mg g^{-1} for laboratory solution. The value for laboratory solution is larger than that obtained in batch tests, 20 mg g^{-1}, as expected (Guimarães, 2010), but in the case of AMD effluent it was not verified. It can be explain by the progressing of pH value along the column when AMD effluent is fed. Every moment a new solution is fed into the column and the calcite present in the bone char is rapidly consumed. This make the pH value of the effluent that leaves the column dropped from approximately 8.0 to 2.96 in a few minutes. Another fact that can also prevent the manganese removal in fixed bed is the high concentration of calcium in the effluent resulted from the precipitation with $Ca(OH)_2$. According to Sicupira *et al*. (2012), the mechanism of manganese removal is based on the ion exchange with the calcium present in the structure of hydroxyapatite, so high concentrations of calcium in the effluent may affect negatively the ion exchange of calcium with manganese.

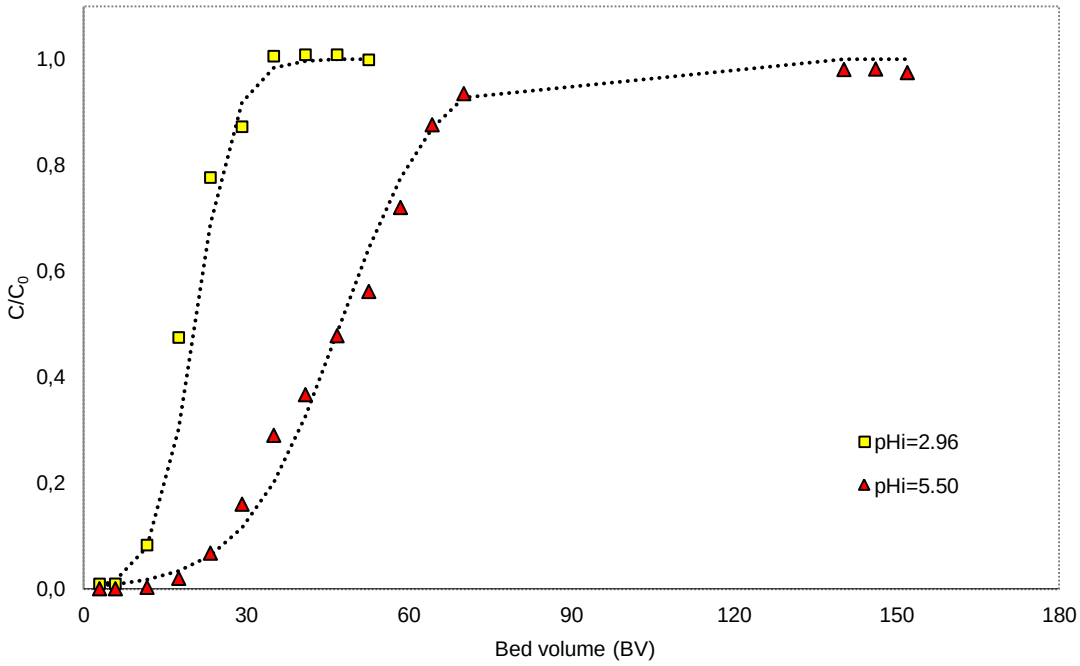

Figure 5.4: Effect of initial pH on the breakthrough of manganese removal with bone char in a continuous fixed bed column using the AMD effluent
(flow rate = 3.0 mL min^{-1}, mass = 20 g, 417-833 µm, continuous curves are Thomas model).

5.3.2 Desorption studies

The design of adsorption processes requires desorption studies to be fully implemented. When the adsorbent becomes exhausted, the recovery of the loaded adsorbent may be advantageous from the economic point of view as much as it can be reused in closed circuit. In fact, regeneration of spent adsorbent columns is quite an important process in wastewater treatment (Mohan and Chander, 2006).

Previous study revealed that manganese adsorption onto bone char occurs as chemisorption (Sicupira *et al.*, 2012). As chemisorption usually results in more stable adsorbed species, desorption is expected to be more difficult to occur. Based on the results shown in Table V.3, the manganese desorption from bone char seems to be not interesting for reusing the material. Using HCl as eluent, the highest desorption obtained was 22.4% with mass loss of 38.8% during 15 minutes of agitation. Using the same conditions but for 5 minutes of agitation, desorption was 21.8% with mass loss of

1.8%. Using H_2SO_4 as eluent, the better result was obtained for H_2SO_4 0.01M with 45.5% of desorption but 36.1% of mass loss after 15 minutes of agitation. Regarding these results, it can be observed that manganese desorption from bone char is not viable due to low desorption levels associated with relatively high mass losses which can even modify the characteristics of the bone char.

Table V.3: Desorption of manganese from loaded bone char using various elution solutions (500 mg, 100 mL, 25°C, 150 rpm, 417-833 µm).

Eluent	Eluent Concentration (mol L^{-1})	Desorption of manganese(%)	Mass loss (%)
HCl	10^{-2}	21.8*	1.8*
	10^{-2}	22.4	38.8
	10^{-3}	6.3	3.0
	10^{-4}	0.0	0.0
H_2SO_4	10^{-2}	45.5	36.1
	10^{-3}	5.2	3.1
	10^{-4}	0.0	0.0
H_2O	-	0.0	0.0

* t = 5 min.

Desorption experiments with bone char loaded with zinc were carried out by Guedes *et al*. (2007). It was observed that desorption with distilled water was not effective but in the case of desorption carried out with the sulphuric acid solution (0.01 mol L^{-1}), the levels of desorption was 40% which can be compared with the level of manganese desorption shown in Table V.3 for the same eluent solution that was of 45%. The authors cited did not report the adsorbent mass loss and desorption experiments with bone char loaded with Mn were not reported.

5.4. Conclusions

In this study, fixed bed tests were carried out to evaluate the feasibility of using bone char for the removal of manganese from AMD effluents in order to reach the maximum

concentration permissible by Brazilian legislation (CONAMA, 2005). Experiments using a laboratory solution containing manganese at typical concentrations were also done for comparative analysis. The following main conclusions can be drawn based on the results obtained:

- For laboratory solution an increase in the mass of bone char increased the number of BV_b which was extended from 11.70 to 34.16. In the case of AMD effluent, increasing the mass of bone char, the BV_b was unchanged due to the other species in solution and/or the precipitate formed on the surface which may limit the removal of manganese.
- Concerning the values of rate constant of Thomas model (k_T) it can be concluded that there are significant variations in resistance to the mass transfer into the bone char for laboratory solutions and AMD effluent. For laboratory solution the mass-transfer zone was almost as long as the bed, so a longer period of time is necessary to reach the saturation point.
- Regarding the influence of flow rate, it was observed that there was no significant change on the number of BV_b. With the increase of the flow rate, the bed was saturated faster. The BV_b was also the same value of 11.70 because it is limited by the number of binding sites.
- Increasing the initial pH of AMD effluent from 2.96 to 5.50, the BV_b was extended from 35.09 to 70.19, as expected.
- The maximum manganese loading calculated in continuous tests using bone char for AMD effluent was 6.03 mg g^{-1} and for laboratory solution was 26.74 mg g^{-1}.
- Manganese desorption tests indicated that reuse of bone char seems to be not applicable. The highest desorption was obtained for H_2SO_4 0.01M with 45.5% of desorption, but 36.1% of mass loss after 15 minutes of agitation. Manganese desorption from bone char is not feasible due to low desorption levels associated with relatively high mass loss which can even modify the characteristics of the bone char.

The removal of manganese from AMD effluents using bone char as adsorbent is technically feasible thus attending environmental legislation, despite desorption seems

not applicable for the eluents solutions investigated. It is interesting to note that bone char may avoid the need for pH correction of effluent after treatment as currently done in the treatment with lime. Also, it can remove fluoride ions and other metals present in AMD effluent (Sicupira *et al*., 2012), so bone char is a quite interesting alternative material for the treatment of AMD effluents**.**

5.5. Acknowledgments

The authors acknowledge the financial support from FAPEMIG, CNPq, CAPES and INCT-Acqua: National Institute of Science and Technology of Mineral Resources, Water and Biodiversity. The contributions from Bone Char do Brasil Ltda and INB (Indústrias Nucleares do Brasil) as well as the fruitful discussions with Prof. Sônia Denise Ferreira Rocha (DEMIN/UFMG) are also kindly acknowledged.

5.6. References

BAMFORTH, S.M.; MANNING, D.A.C.; SINGLETON, I.; YOUNGER, P.L.; JOHNSON, K.L. Manganese removal from mine waters – investigating the occurrence and importance of manganese carbonates. *Applied Geochemistry*, v. 21, p. 1274-1287, 2006.

CAVAS, L.; KARABAYA, Z.; ALYURUKA, H.; DOGAN, H.; DEMIR, G.K. Thomas and artificial neural network models for the fixed-bed adsorption of methylene blue by a beach waste *Posidonia oceanica* (L.) dead leaves. *Chemical Engineering Journal*, v. 171, p. 557-562, 2011.

CHU, K.H. Fixed bed sorption: Setting the record straight on the Bohart–Adams and Thomas models. *Journal of Hazardous Materials,* v. 177, p. 1006-1012, 2010.

CONSELHO NACIONAL DO MEIO AMBIENTE. Resolução CONAMA n.º 357/2005: Classificação dos corpos de água e diretrizes ambientais para o seu enquadramento, bem como estabelece as condições e padrões de lançamento de efluentes. Brasília, 2005. Disponível na Web em: http://www.mma.gov.br/port/conama/index.cfm.

CUSSLER, E.L. Diffusion: Mass Transfer in Fluid Systems. 2nd edition. Cambridge University Press, p. 312-314, 1997.

GONÇALVES, C.R. Remoção de manganês e recuperação de urânio presentes em águas ácidas de mina. Belo Horizonte, 2006. Dissertação (Mestrado) - Centro de Desenvolvimento da Tecnologia Nuclear.

GUEDES, T.S.; MANSUR, M.B.; ROCHA, S.D.F. A perspective of bone char use in the treatment of industrial liquid effluents containing heavy metals. In: XXI ENTMME, Ouro Preto - MG, 2007.

GUIMARÃES, D. Tratamento de efluentes ricos em sulfato por adsorção em resinas de troca iônica. Ouro Preto, 2010. Dissertação (Mestrado) - UFOP.

LADEIRA, A.C.Q.; GONÇALVES, C.R. Influence of anionic species on uranium separation from acid mine water using strong base resins. *Journal of Hazardous Materials*, v. 148, p. 499–504, 2007.

McCABE, W.L.; SMITH, J.C.; HARRIOTT, P. Unit operations of chemical engineering: Chemical Engineering Series. 7th edition. McGraw-Hill´s Science, p. 836-847, 2005.

MOHAN, D.; CHANDER, S. Removal and recovery of metal ions from acid mine drainage using lignite - A low cost sorbent. *Journal of Hazardous Materials*, v. B137, p. 1545-1553, 2006.

NASCIMENTO, M.R.L. Remoção e recuperaçâo de urânio de águas ácidas de mina por resina de troca iônica. São Carlos, 1998. Dissertação (Mestrado) - Universidade Federal de São Carlos.

QUEK, S.Y.; AL-DURI, B. Application of film-pore diffusion model for the adsorption of metal ions on coir in fixed bed column. *Chemical Engineering and Processing*, v. 46, p. 477-485, 2007.

ROBINSON-LORA, M.A.; BRENNAN, R.A. Biosorption of manganese onto chitin and associated proteins during the treatment of mine impacted water. *Chemical Engineering Journal*. v. 162, p. 565-572, 2010.

SICUPIRA, D.C.; SILVA, T.T.; MANSUR, M.B. Batch removal of manganese from acid mine drainage using bone char. *Hydrometallurgy*, submitted, 2012.

UNUABONAH, E.I.; OLU-OWOLABI, B.I.; FASUYI, E.I.; ADEBOWALE, K.O. Modeling of fixed-bed column studies for the adsorption of cadmium onto novel polymer–clay composite adsorbent. *Journal of Hazardous Materials*, v. 179, p. 415-423, 2010.

6. FINAL CONSIDERATIONS AND SUGGESTIONS FOR FUTURE WORKS

In this study, batch and continuous tests were carried out to evaluate the feasibility of using bone char as an alternative material for the removal of manganese from AMD effluents. Experiments using a laboratory solution containing manganese at typical concentrations were also done for comparative analysis. The maximum value of q_m for manganese adsorption based on Langmuir model was 22 mg g^{-1} for batch tests and 6.03 mg g^{-1} for continuous tests. Kinetic tests revealed that manganese removal by bone char is relatively slow and has a relatively small effect of operating variables temperature and particle size. The effect of competing species present in the AMD effluent for the bone char was significant, so the pH of effluent must be raised to near neutral conditions to precipitate the others metals before contact with bone char. Comparing with the current treatment of AMD effluents by precipitation with lime, a smaller volume of sludge is expected. According to Carvalho *et al*. (2009), the removal of manganese at pH close to the neutrality reduces by 50% the volume of precipitate generated in the treatment of the effluent. The removal of manganese from AMD effluents using bone char as adsorbent was technically feasible, but the removal rates of manganese need to be increasing for to be applied in the industry. However, it is interesting to note that the bone char may avoid the need for pH correction of effluent after treatment and can also remove the fluoride and the others metals present in AMD effluent. Manganese desorption from bone char is not applicable due to low desorption levels associated with relatively high mass loss which can even modify the characteristics of the bone char.

On the regard to such final considerations and given the results obtained so far with this work, the following aspects are suggested for future investigations:

1) Evaluate the use of another precipitating agent instead of $Ca(OH)_2$ to increase the pH of the effluent and do a comparative analysis.
2) Evaluate the performance of bone char at manganese adsorption in continuous tests with the effluent pH_i= 7.0.

3) Investigate the chemical characterization of bone char after adsorption in fixed-bed systems in order to identify the compounds formed on the surface that blocked the binding sites.

4) Monitor, during the column experiments, the sorption of the sulfate and fluoride anions onto bone char.

5) Perform a comparative economic evaluation between current treatment of AMD with lime and bone char in columns.

6) Quantify the contribution of the external mass transfer effect on the manganese removal at changing operating conditions.